

Development and Demonstration of an Integrated Tool for Mapping, Sizing and Evaluation of SCC for Remaining Strength Prediction

DOT Contract DTPH56-08-T-000005

Project No. 239

FINAL REPORT

July 8, 2011

Sponsors:

DOT/PHMSA

**Pipeline Research Council International
Washington, D.C.**

Technical Monitor:

James Merritt

303-683-3117

Mark Piazza

PRCI, Inc

Prepared by:

Applus RTD

RTD Quality Service USA L.P.

Houston, TX USA

Principal Investigator:

Martin Fingerhut

Applus RTD

RTD Quality Service USA L.P.

Houston, TX USA

Title:	Development and Demonstration of an Integrated Tool for Mapping, Sizing and Evaluation of SCC for Remaining Strength Prediction
Date:	July 2011
Distribution:	USDOT R&D, PRCI Inc O&I Committee
Prepared By:	Martin Fingerhut and Hamood Rehman
Checked By:	Richard McNealy
Authorized By:	DOT Contract DTPH56-08-T-000005 PRCI Project SCC-2-8, Operations and Integrity Committee
Issued By:	Applus RTD RTD Quality Services USA , L.P. 11801 South Sam Houston Parkway West Houston, TX 77031 Tel: (832) 295-5000 Fax: (832) 295-5001 Martin.Fingerhut@applusrtd.com
Issue No.	V 1

PRCI Version Control			
Ver sion	Date of Last Revision	Date of Uploading	Comments
0	March 31, 2011	April 11, 2011	Draft Report Submitted for Review
1	July 8, 2011	8 July 2011	Final
2			
3			

Disclaimer

This report is furnished to the U.S. Department of Transportation, (DOT), and Pipeline Research Council, Inc. (PRCI) under the terms of OTA DTPH56-08-T-000005 between DOT and RTD Quality Services USA, L.P. (Applus RTD) and PRCI contract PR-366-083505 between Applus RTD and PRCI. The contents of this report are published as received from Applus RTD. The opinions, findings, and conclusions expressed in the report are those of the authors and not necessarily those of PRCI, its member companies, or their representatives. Publication and dissemination of this report by PRCI should not be considered an endorsement by PRCI of Applus RTD, or the accuracy or validity of any opinions, findings, or conclusions expressed herein.

In publishing this report, PRCI and Applus RTD make no warranty or representation, expressed or implied, with respect to the accuracy, completeness, usefulness, or fitness for purpose of the information contained herein, or that the use of any information, method, process, or apparatus disclosed in this report may not infringe on privately owned rights. PRCI and Applus RTD assume no liability with respect to the use of, or for damages resulting from the use of, any information, method, process, or apparatus disclosed in this report.

The contents of this publication, or any part thereof, may not be reproduced or transmitted in any form by any means, electronic or mechanical, including photocopying, recording, storage in an information retrieval system, or otherwise, without the prior, written approval of PRCI.”

Pipeline Research Council International Catalog No. L5XXXX

Copyright, 2011

All Rights Reserved by Pipeline Research Council International, Inc.

This page intentionally left blank

EXECUTIVE SUMMARY

Despite various efforts, no reliable tools and techniques exist in the industry that enables a pipeline operator to quantify the impact of an SCC (Stress Corrosion Cracking) colony on the safety, integrity and reliability of a pipeline. Furthermore, non-destructive tools for reliable detection and measurement are also not available. This forms a huge gap in the state of the art versus the needs of the pipeline industry. Recent developments in technology promise that given a concentrated effort, various components can be integrated to form a comprehensive solution for the pipeline industry.

This research was sponsored by the government and the industry, to develop a solution to address the complex issue of SCC evaluation in the field. Completion of this project resulted in the availability of an integrated tool approach capable of measuring and evaluating SCC as found in pipelines.

SCC has been a formidable challenge to the pipeline industry for over three decades now. Development of a practical solution for measurement and evaluation of SCC has been marred by the complexity of the crack shape and distribution, and the lack of non-destructive technology capable of reliably measuring the crack depths.

Furthermore, application of complex evaluation criteria also requires a lot more detailed measurements than the current practice of using magnetic particle testing can provide.

This research was the final step in a series of efforts geared towards solving this issue. The objective of this research was to develop an integrated tool capable of:

- Detection and mapping of SCC as found in pipelines using the MWM array sensors.
- Depth sizing of the cracks found using Laser ToFD.
- A data analysis tool for identifying the most significant SCC cracks and burst pressure prediction.

The research also included the validation of such evaluation using full scale burst tests.

The risk associated with falsely accepting defects detected on pipelines as safe depends on the knowledge of the accuracy inherent in the applied failure criteria used to predict fitness for service and the effects of assumed versus measured inputs to the criterion and the level of accuracy associated with the measurements. Manufacturing techniques for the production of analog SCC flaws are not available to industry; therefore actual SCC cracks are the only available source of validation data for both the remaining strength criteria and any instruments used to measure SCC (NDE or ILI). Knowledge of the accuracy for measurements of validation flaws is essential in order to understand the true performance of the underlying remaining strength criterion or the true performance of tools such as in-line inspection.

This research deployed an integrated SCC assessment tool consisting of depth screening and crack mapping technology (MWM-Array), a data analysis tool for identifying the most significant SCC crack fields and features on pipe, and Laser ToFD ultrasonic depth sizing. These technologies were previously selected and developed by prior research demonstrating their potential to solve SCC measurement accuracy issues associated with the morphology of SCC.

In order to successfully screen candidate pipe samples in order to insure significant SCC was identified and tested a protocol using MPI, a qualified phased array ultrasonic NDE procedure and severity assessment by API 579 FAD was employed. The validation pressure tests revealed the phased array sizing to be consistent with the pre-qualification with equal performance from the Laser ToFD, however, the sample population was not sufficient to determine a complete performance specification. Additional validation tests where actual SCC flaw dimensions are determined from fracture surfaces would be required in order to determine confidence intervals. Binomial distributions indicate that a sample of population of 14 comparisons are required in order to obtain a full confidence interval at a certainty of $p=0.8$ with 95% confidence.

This research did demonstrate the protocol necessary to screen candidate pipe to insure candidate pipe fails at target SCC indications and not at mill damage locations or at other integrity conditions. Extraction of additional comparisons by freezing and breaking SCC indications for depth confirmation was also demonstrated by this research and could be utilized for increasing the validation population for crack dimensions. Based on the experience from this research the numbers of candidate pipes for validation pressure tests would have to be significantly larger than the minimum number of required test samples to account for rejection due to the presence of mill/manufacturing flaws. The SCC-2-8 research was also limited in the number of pipelines from which pipe was sourced and as a result the variety of SCC morphologies was also limited.

Further testing of the integrated tool approach to SCC assessment for the purposes of completing a full performance specification is recommended based on the promising results from the integrated tool and screening protocol. Additional fitness-for service criterion, such as Corlas, PAFFC and BS 7910 could be included in the research in order to critically compare the level of accuracy afforded by all the current axial crack assessment models. Pipe should be sourced from both liquid as well as gas pipeline operators with the objective of testing crack representing both near neutral and high pH SCC.

INTRODUCTION

The research presented here represents the development, application and validation of an integrated NDE tool and process for characterizing the effect of Stress Corrosion Cracking (SCC) on pipelines,

addressing known difficulties relating to accuracy of crack measurements within SCC crack fields using current technologies. The Pipeline Research Council International (PRCI) together with the Pipeline and Hazardous Materials Safety Administration of the U.S. Department of Transportation (USDOT) sponsored the research to develop and validate an integrated tool and process to directly measure SCC on real pipelines, characterize the features, predict failure pressures using current available pressure assessment criteria and validate the results against hydrostatic burst test of the pipe. This research was based on prior work investigating the fundamental physics and proof of concept for the application of the an ultrasonic NDE technology known as laser based time of flight diffraction (LToFD) ultrasonic testing and eddy current based meandering winding magnetometer (MWM[®]-Array) technology to the assessment of SCC cracks in pipe. [1], [2]

An important aspect of integrity management for pipelines involves the detection and characterization of conditions affecting pipeline integrity, such as metal loss cracks and dents to determine safe operating parameters. For pipe wall metal loss due to corrosion, criteria have been developed, validated and cited in codes and regulations to predict remaining strength for corroded pipe. [9] Those criteria have been widely and successfully applied by industry to justify pipe repair or replacement decisions. The directly applied non-destructive examination (NDE) technologies for measurement of pipe wall metal loss have been demonstrated to be highly accurate and together with years of practical application and validation testing by the industry, a high level of reliability has been demonstrated.

ILI metal loss technologies incorporate the accepted remaining strength criteria thus allowing pipeline operators to prioritize selection of locations for excavation and direct (NDE) based on those ILI predictions. The knowledge of the true detection and characterization performance of ILI technologies allows for determination of the risk level associated with accepting ILI predictions and industry standards have been developed providing guidance to industry. [3]

Other threats to pipeline integrity can result from cracks in the wall of pipe and research efforts continue within the pipeline industry to develop and understand the reliability of remaining strength criteria for those conditions. ILI technology development for tools with the capability to detect and discriminate cracks has also continued. The objectives of these continued industry development efforts are to insure reliable integrity management of the threats known to cause cracks. SCC is one specific threat known to result in pipe wall cracks. Prior research and industry experience has identified issues affecting detection and discrimination accuracy of current NDE technologies for pipe wall cracks due to SCC. Those issues arise from the tendency for SCC to occur within colonies containing multiple cracks with small side to side and tip-to-tip separation, and the thru wall shapes of SCC cracks, which can result in NDE measurement accuracy different from singular cracks caused by other threats. Industry application of current NDE technologies to SCC has demonstrated that detection and discrimination accuracy can vary significantly

depending on the specific technology and operator skill and level of training. [4] The accuracy of thru wall crack depth measurement and measurement of the spatial relationship of individual crack lengths, and separation within SCC crack fields affects the accuracy of burst pressure failure predictions using the prediction criteria available to industry such as Modified Ln-Sec, API RP 579 FAD, BS 7910 and others. Cracking revealed during direct examination is normally replaced or ground/buffed out in accordance with established procedures, although industry has proposed changes to Code for gas pipelines to define a category for shallow depth SCC that may be re-coated and returned to service without grinding/buffing. [5] Grinding/Buffering is specified industry standard practice for determining crack thru-wall depth compared with ultrasonic NDE techniques such as manual ToFD, Near Side Detection and Sizing (NSDS) and phased array sector scans recognizing their need for robust inspection procedures to insure reliability. [4] The known limitations of conventional NDE for sizing SCC cracks could inhibit widespread application of the proposed SCC mitigation standards representing a motivation for the development of an SCC assessment tool providing cost effective and accurate assessment of SCC type cracks.

ILI crack tool technologies have been developed to assess SCC in pipelines. The current technologies predict locations of cracks, both axially and circumferentially with various levels of depth and axial length discrimination. However, the ILI crack tool technologies have not developed to the point where severity discrimination and prioritization based on burst failure pressure prediction can be provided to the same extent as enjoyed by the ILI technologies used to manage metal loss threat. Understanding true ILI crack tool sizing performance and the relationship of that performance to the reliability of burst failure pressure predictions will allow more successful application of ILI in response to the threat of SCC. ILI crack tool development and improvement has depended upon the comparison of ILI predictions with actual conditions found in the field resulting from actual ILI crack tool runs. If the accuracy of the field validation NDE is significantly better than the prediction accuracy of the ILI tool then the true performance of the ILI tool can be discerned directly from field comparisons without correction, otherwise the field NDE sizing accuracy must be known and prior research has shown to offer special challenges. [6]

The aim of this research was to integrate data from promising technologies identified by the prior research (LToFD and MWM) thus improving error in measurement of cracks within SCC fields and compare predictions of crack sizing and burst pressure with hydrostatic burst tests. The realization of an SCC assessment tool with improved accuracy and reliability compared with current practice would aid industry in the identification of reliable pressure assessment failure criteria, assist ILI vendors in the improvement of their technology and improve pipeline operator's ability to improve pipeline reliability with respect to SCC threat.

PRIOR RESEARCH

The current industry practice to evaluate the extent and severity of SCC identified by ILI or hydrostatic test failures is to employ a direct examination protocol consisting of magnetic particle inspection (MPI). There are number of available MPI procedures described in NACE SCC Standard Practice SP0204 [6] with black on white contrast type being the most widely applied. MPI indications allow for the location, length and spacing of SCC to be documented, but cannot reveal depth. The effectiveness of MPI was evaluated during the course of a Joint Industry Project [2] and shown to be reliable for documenting location length and spacing of SCC cracks but recording of results rely on photography and manual digitization of crack dimensions. The work of the JIP was in co-operation with JENTEK Sensors Inc (JENTEK) who at the time was conducting research funded thru the USDOT Small Business Innovation Research (SBIR) Program. That research resulted in proof of successful adaptation of the eddy current based JENTEK MWM-Array technology to high resolution surface mapping of SCC cracks providing digital dimensional measurement and data logging with performance matching or exceeding MPI. [7] Additionally the potential for the MWM-Array technology to identify crack depths of 10% of wall thickness was investigated and proposed as a candidate for later research and development. The depth measurement capability of the MWM-Array for SCC cracking is in the early development stages and is being funded separately by the USDOT.

The depth of SCC cracks can, in principle, be measured using ultrasonic shear wave techniques; however, the typical proximity of nearby cracks within SCC colonies (fields) can cause interference that can lead to erroneous readings. Time of Flight and sector scan phased array ultrasonic technology applied to SCC sizing was the subject of early research. The conclusions were that the complexity of SCC defects produces problems for ToFD in the measurement of SCC crack depth in thin wall pipe but possible if robust qualified inspection procedures are followed. [8] That same study concluded phased array ultrasonic technology (PA) is effective for imaging and sizing SCC in natural gas pipelines. Subsequent industry experience using PA for sizing SCC (confirmed by grinding) has confirmed that measurement accuracy suitable for use in assessing burst pressures and validating true ILI performance can be obtained but dependent on operator skill, training and experience.

Research was conducted in 2007 and 2008 by Intelligent Optical Systems, Inc (IOS) together with Applus RTD, co-funded by the USDOT/PHMSA and PRCI [1], to apply proven laser based LToFD ultrasonic technology and finite difference modeling to SCC cracks. The objective was to determine if the rich admixture of ultrasonic wave types, directions and frequencies together with the small application foot print possible with laser delivery could provide accurate sizing of SCC cracks addressing the known gaps from application of conventional ultrasonic NDE.

Laser based ultrasonics is an established non-contact NDE technology. Lasers can be used to generate and detect ultrasonic waves within the wall of pipe. It is a non-contact technique consisting of a generation laser, detection laser and a receiver. The principle for laser generation of ultrasonic waves in solids relies on the principle of thermal expansion or ablation with ultrasound generated by the sudden thermal expansion of a small surface spot. The generation laser power can be increased to the point where some surface material is evaporated and ultrasound is generated by the recoil effect of the expanding evaporated material. When scattered or reflected waves within the material return to the surface, the resulting vibration is detected with a separate laser receiver. The ToFD approach using laser ultrasonics (LToFD) has some unique properties compared with TOFD using conventional ultrasound techniques for crack sizing. First, there is a choice to optimize shear waves, longitudinal waves or both. Second, the large frequency range for generated waves improves the likelihood of significant diffraction for a range of crack properties. Cracks are typically located in the near field of the generated waves (at lower frequencies) so a geometric ray tracing approach is too simplistic and finite difference calculations were performed to validate the LToFD approach. A conceptual diagram illustrating the application of generation and detection lasers and predicted wave propagation is shown in **Figure 1**. The small laser beam spot size on the pipe surface allows placement of both ultrasound generation and detection within close proximity to individual cracks thus making it possible to measure individual cracks within complex colonies. The numerical simulations from the prior research demonstrated that no useful information can be obtained from ToFD by straddling an entire SCC colony necessitating the location of ultrasound generation and detection in close proximity to individual cracks within colonies as afforded by the Laser ultrasonic technique (LToFD).

Additional simulations in the prior research also demonstrated that thru-wall curvature of cracks can have an effect on arrival of diffracted tip signals indicating some control of crack-to-beam distance tracking would be required. This behavior lead Applus RTD to later investigate the potential applicability of LToFD for the detection and characterization of bond area flaws in longitudinal welds made by electric resistance welding (ERW) which have been known to exhibit hook crack conditions. Given the ability for greater latitude for spacing LToFD beam spots compared with SCC applications the potential for application of LToFD to ERW flaws has been investigated and future research is anticipated. That prior research concluded with a successful demonstration of the LToFD technique applied to SCC samples and identified the process variables to be considered for successful development and application as an SCC inspection and assessment tool. [1]. So far the LToFD technique has not been applied to other bond line defects such as cold welds, stitching, etc. Whether these can be detected with LToFD is therefore unknown.

INTEGRATED TOOL DEVELOPMENT

In view of promising results from the prior research, Applus RTD, in cooperation with IOS and JENTEK was co-sponsored by USDOT/PHMSA and PRCI to investigate the integration of the LToFD and MWM technology into a tool and process with capability to practically assess SCC under field conditions. The physical measurement data from the sensor technologies were to be evaluated using recognized crack assessment methodologies as described in the USDOT/PHMSA Stress Corrosion Cracking Study TTO Number 8 in order to predict the effect of SCC on the pressure boundary of pipe. The accuracy of crack measurements on pipe and the effect of measurement error on pressure assessment predictions would be observed through a series of trials applying the integrated technologies to measurement of actual SCC found on operating pipelines during the course of ILI assessments. The pipe, with SCC locations would be subsequently subjected to hydrostatic test to failure. From the observations of actual SCC dimensions on fracture surfaces comparisons with predicted dimensions from NDE were possible together with comparisons of actual failure pressure with that predicted by the pressure based assessment criteria. Multiple pressure based assessment criteria are cited by the current SCC guidance documents, including; NG-18 Ln-Sec, Corlas, PAFFC, and API RP579. [4] The use of API RP579 Level II Failure Assessment Diagram (FAD) pressure based assessment criterion was proposed for this research since it represents a public domain methodology, although for comparison another public domain methodology, the NG-18 Modified Ln-Sec approach was also used. Blade Energy Partners Ltd collaborated in this research to manage both the integration of the measurement data into the pressure based assessment model and hydrostatic burst tests.

At the conclusion of the prior research by IOS and RTD a functional specification for a practical system to assess SCC on pipelines was proposed based on crack measurement issues experienced during the course of the research and conceptual demonstration. Additionally, Applus RTD identified systemic considerations recognizing practical pipeline inspection requirements. A possible link was identified with the prior research and JIP concerning the MWM-Array^(R) crack mapping technology. This formed the basis for the integration of the technologies and a proposed physical platform.

It was recognized in the prior research that the occurrence of SCC on pipes can involve multiple cracks and crack fields within individual excavation sites and that the inspection speed for LToFD would preclude the economical application of the technology. The eddy current based MWM-Array sensor was identified as having the potential to map surface cracks and the possibility to screen for cracks greater than 10% wall thickness thus offering the potential for identifying "significant cracks" for subsequent measurement by LToFD. Within the current research, JENTEK developed a crack depth algorithm to be used in conjunction with the FA28 MWM-Array measurements. The deepest penetrating frequency for that sensor results in a thru thickness field penetration of 0.02 inches which is approximately 10% wall thickness for 0.200 inch wall pipe. However, the actual depth of sensitivity

to crack depth will vary with crack morphology (i.e. width). Preliminary experiments conducted involving the scanning of pipe samples with SCC using the JENTEK FA28 MWM-Array sensor, consecutively grinding, re-scanning the samples with MWM-Array and observing changes in the conductivity scan. This data will be used to support further development of the MWM-Array crack depth capability. Separate DOT funded research was reported by JENTEK relating to development of a deep penetrating very low frequency array probe that should enable crack measurements to depths greater than 0.1 inches. Multiple trials by Applus RTD with the JENTEK MWM-Array documented the detection limits for SCC cracks compared favorably with black on white MPI [2]. A comparison of results from MPI with MWM-Array is shown in **Figure 2** showing 95% of the time the error was between -0.017 and 0.003 inches.

The MWM-Array sensor was integrated into a scanning platform as shown in **Figure 3** which enables scanning in both circumferential and axial directions on the external pipe surface. The MWM-array creates a digital record of crack indication centerline coordinates thus providing a source of tracking coordinates for use by LToFD for necessary precise spacing from cracks.

Several issues were identified by the prior research relating to the LToFD technology applied to SCC cracks and incorporated into the integrated tool for the current research. The fiber bundle that was used in the prior research for delivery of the ultrasound generation beam was replaced by a single 1mm core fiber. That fiber enables the delivery of up to 50 mJ of laser energy compared with about 10mJ with the fiber from the previous research. The larger fiber core necessitated the use of a shorter focal length objective lens in order to preserve a small laser spot size on the pipe surface. The lens change also required other changes to the internal optics in order to maintain the 4 to 5 mm separation between the generation and detection laser spots on the pipe surface that was identified as an essential variable in the previous research.

A fiber combining module was added to the back of the inspection head combing the three fibers into a single cable or bundle between the inspection head and the controllers and laser generators.

A 10 W detection laser replaced the 2W probe laser used in the prior research where pipe surface roughness was thought to contribute to low collected signal power and light surface grinding of the pipe surface near the cracks to enhance reflectivity. It was thought that a higher power detection laser would allow the demodulator to function in the current research with highest signal-to-noise.

The band scanner technology from automated weld inspection with two flexible metal bands clamped around the outside diameter of the pipe and axial scan rail mounted between those bands was retained from the prior research. Linear actuator motors are affixed to the ends of the scan rail and clamped by drive wheels to the circumferential metal bands providing circumferential motion. A

motorized lead screw is mounted onto the scan rail drive and provides axial motion for the sensor packages. A motor controller is programmed with crack centerline coordinates obtained from a MWM-Array scan of a pipe surface segment. Since SCC cracks are known to coalesce into non-axial configurations it was necessary to provide a motor controller capable of accepting and following high resolution coordinates, both axial and circumferential from the MWM-Array in order to keep the LToFD beams optimal beam offset of 1.25 to 1.5 mm from the crack centerline. A data conversion routine was required for the transfer of MWM-Array data to the scanner motor controllers. Repositioning repeatability of the scanner must be maintained to within +/- 0.75mm in order to maintain beam spacing along the crack path. **Figure 4** contains photographs of the improved inspection head and fiber optic cable bundles.

The tendency for individual SCC cracks to interact (coalesce) within crack fields is dependent on the circumferential and axial separation between individual (or interlinked) cracks as defined by CEPA and NACE RP0204. The maximum crack length and path, including interlinking and interacting cracks can be determined by application of the crack separation criterion to the crack maps provided by MWM-Array scans. Digitization of the maximum crack lengths are fed to the motor controller enabling tracking of the LToFD lasers for the length of the crack.

Crack depth measurements by LToFD along the maximum crack path lengths can be evaluated by the pressure assessment methodologies (API RP579 Level II FAD and NG-18 Modified Ln-Sec) to predict the remaining strength of pipe with SCC. Software routines have been developed and are available that can provide pressure assessment in-ditch concurrent with crack dimensions. These pressure assessment criteria do not require measurement of other material properties using specified minimum yield strength and assumed values for pipe fracture toughness that can be estimated from knowledge of pipe vintage, manufacturer and grade.

A schematic illustrating the integrated tool functional specification consisting of crack surface mapping, LToFD measurement and crack assessment is shown in **Figure 5**.

FIELD TRAIL AND VALIDATION

Pipes with SCC indicated by ILI were supplied by PRCI member companies as an in-kind contribution to the research effort. A total of 15 pipe samples from 13 pipeline dig sites representing two pipelines (34 inch x 9.5 mm, X-52) were obtained. This pipe contained typical examples of indications predicted by ILI for which in-ditch field assessment would be required and represented the field trial opportunities for the integrated SCC assessment tool. These pipe samples were subjected to preliminary conventional NDE by the pipeline operators prior to removal from the operating pipelines to confirm the

presence of SCC. The research project planned to obtain a sufficient quantity of pipe with “significant” SCC for assessment by the integrated tool and hydrostatic test to failure of eight (8) pipe sections in order to provide validation comparison of predictions made using the tool. This objective presented several challenges compared with the performance of strict “field trial”. In pressure testing a pipe specimen to failure it must be free of other defects such as corrosion or manufacturing defects that would be prone to failure before any SCC reached a point of failure. In addition, SCC severity can be low enough that pipe samples can plastically expand beyond the capability of test configurations to induce a meaningful failure in the absence of other defects. Given the potential for these issues it was necessary to subject the validation pipe population to full 360 degree screening using black on white MPI in order to screen the pipes for all SCC and manufacturing defects such as pipe wall laps, seams, scabs, slivers and seam weld surface connecting lack of fusion or cracks. This level of NDE is not typical of conventional field NDE protocol. Table 1 summarizes level of detailed screening and results necessary to obtain 5 pipes with significant SCC for further testing.

From the population of available pipe consisting of 15 individual lengths of pipe suitable for hydrostatic pressure testing, 3 pipes had weld seam toe cracks. Of the remaining 12 pipes, 3 pipes did have SCC but also exhibited weld toe seam indications. Preliminary hydrostatic tests of those pipes indicated the seam weld manufacturing defects failed before any of the SCC indications. One pipe had low level (20% wall thickness depth) SCC but significant using the API 579FAD criterion and that pipe was subjected to pressure test in order to validate the screening approach. This left 4 pipes with SCC indications to be considered for validation of the integrated SCC tool using LToFD.

Since the remaining four (4) pipes contained multiple SCC indications and colonies the use of the proposed industry criterion mentioned earlier for “significant SCC” based on thru wall depth greater than 10% wall would not be sufficient to predict failure locations using the MWM-Array crack depth algorithm. Also, as mentioned earlier, the application of LToFD for sizing every SCC indication on all pipes would be economically un-feasible. Therefore, an additional screening step was implemented for the research, namely the use of a qualified phased array ultrasonic technique to screen all the SCC crack fields for thru wall depth profile. By combining the maximum crack lengths from the MWM-Array scans with the phased array ultrasonic depth profiles a severity ranking for all SCC could be predicted using the API RP 579 FAD criterion. The most severe cracks identified by the screening were selected for depth profile measurement by LToFD and final prediction of remaining strength.

The inspected pipes containing the SCC indications had their ends closed off by butt-welding of dished end caps and the assemblies were filled with water and subjected to increasing internal hydrostatic pressure until the assemblies leaked or ruptured. The most severe crack location, identified by the screening process, on each test sample was instrumented by strain gauges and observed using high speed videography. Figure 6 shows the configuration for pipes prepared for hydrostatic test and the

arrangement of pipes within the pressure test cell at Texas A&M University who conducted all pressure test-to-failure under the direction of Blade Energy Partners, Ltd. **Table 1** summarizes the results from the hydrostatic tests.

VALIDATED CAPABILITIES

All of the samples with “significant” SCC either leaked or failed at pressures greater than 110% SMYS indicating the available population would have survived hydrostatic integrity test. The resulting fracture surfaces were examined and actual SCC crack depth profiles and interacting total crack length at failure were measured.

Figure 7 shows the MWM-Array crack map from the most significant SCC crack field found on Pipe # 4 together with the maximum crack length predicted by the extent of axial interaction determined in accordance with the NACE/CEPA criterion. Based on the maximum crack length measurements and PA ultrasonic depth screening the most severe interacted crack was identified based on API RP 579 FAD criterion and noted as the target crack #32 in Figure 7. LToFD depth measurement was performed on the target crack and the ablation track from the generation laser in relation to the target crack are shown in **Figure 8** together with the depth results obtained from LToFD, PA screening and the actual depth profile for SCC obtained from the fracture surface resulting from the hydrostatic test to failure.

A total of six pipes were subjected to screening using MPI, PA and API 579 severity ranking. Two of the six pipes were selected for hydrostatic test to failure in order to validate that the protocol would identify the significant crack likely to fail when multiple cracks and crack are present. For those two pipes one ruptured at the significant crack identified by the protocol while the second pipe had predicted SCC greater than 10% wall thickness but very short length and that pipe was pressured to 140% SMYS resulting in significant expansion without rupture or leak and that test was terminated. The significant cracks identified in the four (4) remaining pipes were subjected to LToFD and detailed PA depth mapping. Three of the four target crack locations failed by leak or rupture with failure for the fourth pipe (Pipe #10B) by leak at another SCC location other than the target. For pipe #10B sections were taken at the target locations, frozen and broken to reveal the actual SCC crack dimensions for comparison with the LToFD and PA predictions.

A unity plot comparing the LToFD and PA depth size predictions is shown in **Figure 9**. The mean error (ILI-Actual) for the test population was non-conservative for both PA and LToFD (-0.08 mm for PA and -0.83 mm for LToFD influenced by the presence of two non-conservative outliers. Pipe #13, crack 13A represented the most significant undercall for both PA and LToFD. Pipe #10A exhibited a comparison outside of +/- 1.0mm for LToFD while PA estimated the depth well for the significant SCC crack. It was

noted during the trials that pipe surface roughness, due to low level external corrosion associated with the SCC (may be a characteristic of near neutral pH SCC) was observed and LToFD experienced some loss of data similar to the experience in the prior research. External surface grinding with 180 grit abrasive did provide sufficient signal-to-noise but in some instances the lack of signal could also have been due to ultrasonic transparency of the cracks related to crack width or crack tip morphology characteristic of SCC.

The maximum interacted crack length was determined by using the crack tip to tip and end to end separation specified by NACE RP0204 using commercially available software where digital representations of the crack fields (either MWM or MPI) can be scaled and interacting cracks identified. **Figure 10** is a unity plot comparing the predicted interacted crack lengths with the actual maximum crack length observed on the fracture surfaces from the test pipes. Photographs of the fracture surfaces are provided in Annex A and interacted maximum length determined by measurements from both MPI and MWM-Array crack surface maps shown in **Figure 7** for Pipe 4 and the other test pipes also provided in Annex A.

The use of API 579 Level II FAD with an assessment toughness of 50 ft-lbs upper shelf Charpy v-notch impact energy, results in a limiting safe pressure that was used within the context of the integrated tool/process for the identification of significant cracks for sizing using LToFD. In all instances the API 579 Level II FAD limiting safe pressures were less than the hydrostatic pressure test failure pressures. In order to investigate the sensitivity of the NDE measurements on the predictions of failure pressure for comparison with actual test failure pressures a different criterion was employed, namely NG-18 Mod Ln-Sec criterion. **Figure 11** is a unity plot comparing the failure pressures predicted by NG-18 Mod Ln-Sec using PA and ToFD sizing and from dimensions obtained from fracture surfaces (assuming 50 Ft-lbs Charpy V-Notch toughness) with the actual failure pressures. The results are conservative as expected using the NG-18 criterion. More accurate failure pressure results may be provided by the other recognized criteria; API 579 Level III, Corlas or PAFFC but were not considered for this research.

Considering the population of errors for failure pressure prediction based on NDE measurements (Prediction-Actual), the average error for the failure pressure predictions was -294 psi indicating a conservative bias with a standard deviation of 85 psi. The standard deviation of 85 psi means that 99.5 percent of the data would be expected to lie within 255 psi of the distribution mean. Considering the population of errors for failure pressure prediction based on actual fracture surface measurements (Prediction-Actual), the average error for the failure pressure predictions was -258 psi indicating a conservative bias with a standard deviation of 91psi. The standard deviation of 91 psi implies that 99.5 percent of the data would be expected to lie within 273 psi of the distribution mean. The difference in these distribution statistics illustrates the effect of the NDE measurement errors.

DISCUSSION

MWM-Array did not demonstrate the capability to identify and screen out cracks less than 10% wall thickness due to the fact the MWM-Array sensor available at the time and used in this research was unable to penetrate pipe wall beyond 0.02 inch wall thickness (5% wall thickness for pipe samples). Industry proposals have identified that cracks less than 10% wall thickness may not pose a significant threat to gas pipeline integrity and therefore the need for a technology having the potential for screening SCC populations for crack depth. For the current research, since SCC populations may often contain cracks greater than 10% wall thickness an additional capability for screening deeper cracks was shown to be required and PA ultrasonic technology was selected. The success rate for the identification of the most significant cracks on the pipe samples indicated that the depth screening accuracy afforded by the PA ultrasonic technique is required in order to reliably discriminate crack severity using crack depth measurements.

To support field SCC rehabilitation decisions, the integrated tool as tested here would also require a supplemental depth screening capability, such as PA ultrasonics to fully discriminate more severe SCC categories. The measurement speed for the LToFD, as identified in the prior research is not suited to economically measure large numbers of cracks and therefore improved or added high speed depth screening capability would be required for the integrated tool concept. The future development of variable very low frequency MWM-Array technology to enable discrimination of flaw depth categories deeper than 10% wall thickness coupled with application of a separate high frequency array, as used in this research, for detailed surface mapping could help control the amount of local grinding/buffing and insure correct application of higher resolution NDE such as PA or LToFD and optimize SCC rehabilitation response to ILI predictions.

The use of MWM-Array demonstrated accurate results for the purposes of determining the individual SCC crack lengths but the industry crack interaction model (NACE/CEPA) resulted in some variability in agreement with the results of total crack length determined from the hydrostatic pressure test fracture surfaces.

The LToFD technology did demonstrate the capability for highly accurate measurement of SCC cracks in most of the tests but issues relating to ultrasonic transparency resulting in non-conservative depth measurement remain. Changes to the LToFD system identified in the prior research did not appear to correct this issue and this research demonstrated the consequence of significant under prediction of SCC crack depth. The depth accuracy results from PA ultrasonic were not inconsistent with results of previous Applus RTD and industry experience applied to SCC.

Based on the pressure test distribution statistics, for failure pressure predictions accepted at a deterministic safety factor of 1.39 (corresponding to a design factor of 0.72), corrected for the conservative prediction bias with an upper bound of more than three standard deviations, (for both NDE predictions and actual values), one can expect that cracks left in a pipeline would be extremely unlikely to fail in service. This same rationale was used to validate the safety of RSTRENG for metal loss from hydrostatic pressure tests-to-failure by Kiefner and Vieth. [9] Validation pressure tests of corrosion metal loss benefited from the relative ease and accuracy of measurements of metal loss and artificial features can be easily manufactured to known dimensions allowing for large validation populations. Validation of crack failure criteria has historically had to rely on measurement of actual flaw dimensions from fracture surfaces, consequently, sources of validation samples have relied on field failures limited numbers of pressure test opportunities and efforts have been constrained by sample size. The protocol demonstrated here appears to have the potential for screening significant sample populations of pipe with SCC for validation pressure testing similar in scope with sample sized comparable to that used previously employed to validate metal loss failure criteria.

The reliability of ILI tools are often demonstrated by comparing their predictions of failure pressure from pull tests conducted on pipe samples with flaws or from direct examination of pipe from operating pipelines inspected by ILI. Those results, considering their bias and variance of predictions against the available pressure based failure criteria (NG-18 Ln-Sec, Corlas, PAFFC or API 579 FAD) can be compared against the inherent bias and variance of the pressure based criteria compared with pressure-to-failure data in order to determine the risk of false acceptance of ILI indications as safe. Manufacturing techniques for the production of analog SCC flaws are not available to industry; therefore actual SCC cracks are the only available source of ILI validation data. The SCC assessment protocol demonstrated here, using either PA ultrasonic or LToFD appears to have potential for predicting both crack dimensions and failure pressures of SCC for comparison against ILI predictions for determining true ILI performance from pull test samples or from field comparison opportunities. Larger failure pressure sample sizes than that available for this research would necessarily be required in order to determine a full performance specification for the protocol.

For the purposes of determining true ILI crack tool performance, length prediction and the ability to document surface interaction afforded by MWM-Array would provide value. The current research did not provide a sufficient number of validation comparisons in order to conclude reliability for predictions based on either PA ultrasonic or LToFD. Additional validation tests where actual SCC flaw dimensions are determined from fracture surfaces would be required in order to determine confidence intervals. Binomial distributions indicate that a sample of population of 14 comparisons are required in order to obtain a full confidence interval at a certainty of $p=0.8$ with 95% confidence. This research did demonstrate the

protocol necessary to screen candidate pipe to insure candidate pipe fails at target indications and not at mill damage locations. Extraction of additional comparisons by freezing and breaking SCC indications for depth confirmation was also demonstrated by this research and could be utilized for increasing the validation population for crack dimensions. Based on the experience from this research the numbers of candidate pipes for validation pressure tests would have to be significantly larger than the minimum number of required test samples to account for rejection due to the presence of mill/manufacturing flaws.

CONCLUSIONS AND RECOMMENDATIONS

- Efforts in the direction of evaluation and fitness for service (FFS) assessment of SCC in pipelines have been marred due to the lack of non-destructive testing technology and subsequently, limited means of validating any FFS assessment methods.
- This research successfully deployed an integrated SCC assessment tool consisting of depth screening and crack mapping technology (MWM-Array and Phased Array), a data analysis tool for identifying the most significant SCC crack fields and features on pipe, and Laser ToFD ultrasonic depth sizing.
- A total of 15 pipe samples from 13 pipeline dig sites representing two pipelines were obtained for this research. NDE inspection and hydrostatic pressure test to failure summary for these pipe samples is listed in Table 1.
- Further testing of this integrated tool approach to SCC assessment for the purposes of completing a full performance specification is recommended based on the promising results from the integrated tool and screening protocol.
- MWM depth screening capability to screen out cracks less than 10% of the wall thickness is still under development and is highly recommended. Phased array Ultrasonics was used as a depth screening tool in this research.

REFERENCES

1. Klein, M., Characterization of Stress Corrosion Cracking Using Laser Ultrasonics, Final Report 0808, DOT Contract No. DTPH56-06-T-000003, PRCI SCC-3-6, Aug 31, 2008
2. RTD Quality Services SCC-JIP Report, " Qualification of Eddy Current MWM Sensor for Detection of SCC, Internal JIP Report referenced within Ref 1, July 2007
3. API 1163, In-Line Inspection Systems Qualification Standard- 2005
4. Michael Baker Jr., Stress Corrosion Cracking Study, Final Report, USDOT/PHMSA DTRS56-02-D-70036 TTO Number 8, January 2005
5. Batte, D., Fessler, R., Rapp, S.C., Severity of Stress Corrosion Cracks in Pipelines - Categories and Responses, NACE2008-Paper No. 08675
6. McNealy, R., McCann, R., In-Line Inspection Performance III, Effect of In-Ditch Errors in Determining ILI Performance, ASME IPC2010-31269, Sept 2010 Calgary AB Canada
7. Goldfine, N., High Resolution Electromagnetic Imaging and Decision Support for Pipeline Life Management, DOT SBIR 2006 Phase I Final Report, DOT DTRT57-07-C-10005
8. Michael Baker Jr., Stress Corrosion Cracking Study, Final Report, pp. 55, USDOT/PHMSA DTRS56-02-D-70036 TTO Number 8, January 2005
9. Kiefner, J. Vieth, P., Roytman, I., Continued Validation of RSTRENG, PRCI L51749, Dec 1996

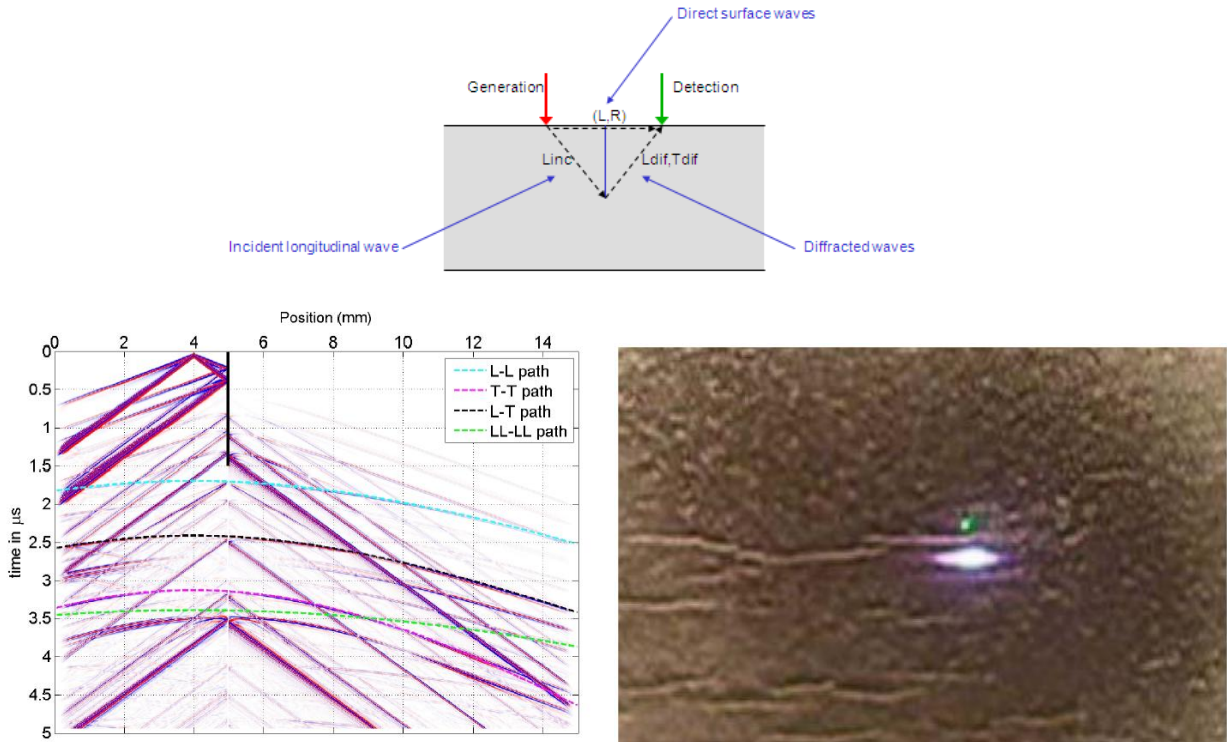


Figure 1: Position of generation and detection lasers with respect to a crack with a B-Scan plot of the normal surface velocity as a function of detection spot position. The photograph shows the laser spots on the surface of a test piece on both side of an SCC crack.

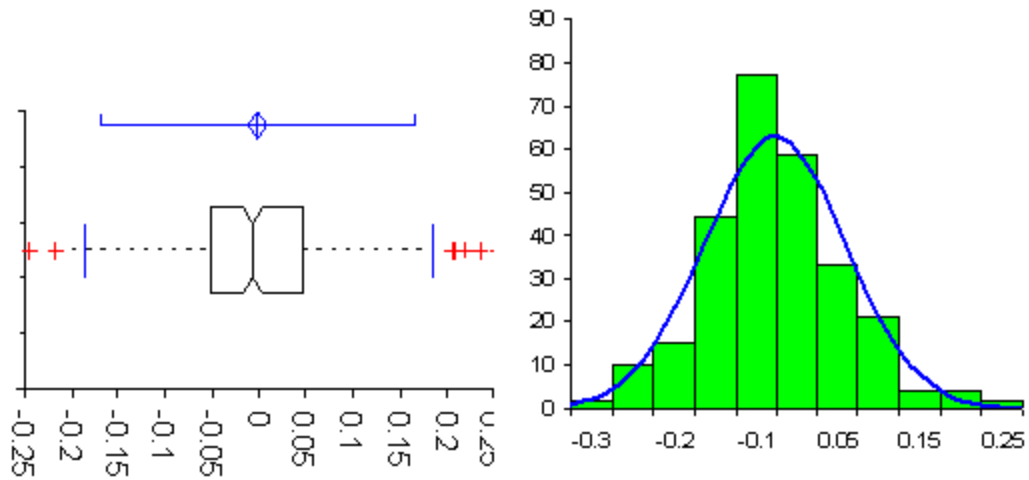


Figure 2: Error distribution for MPI vs MWM-Array crack length measurements.

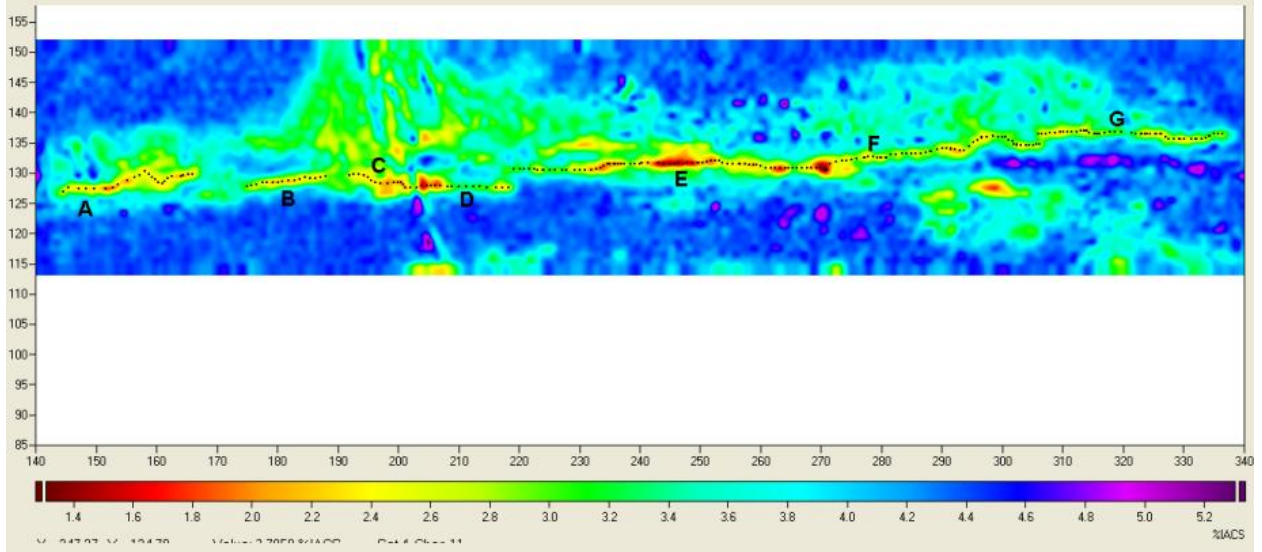
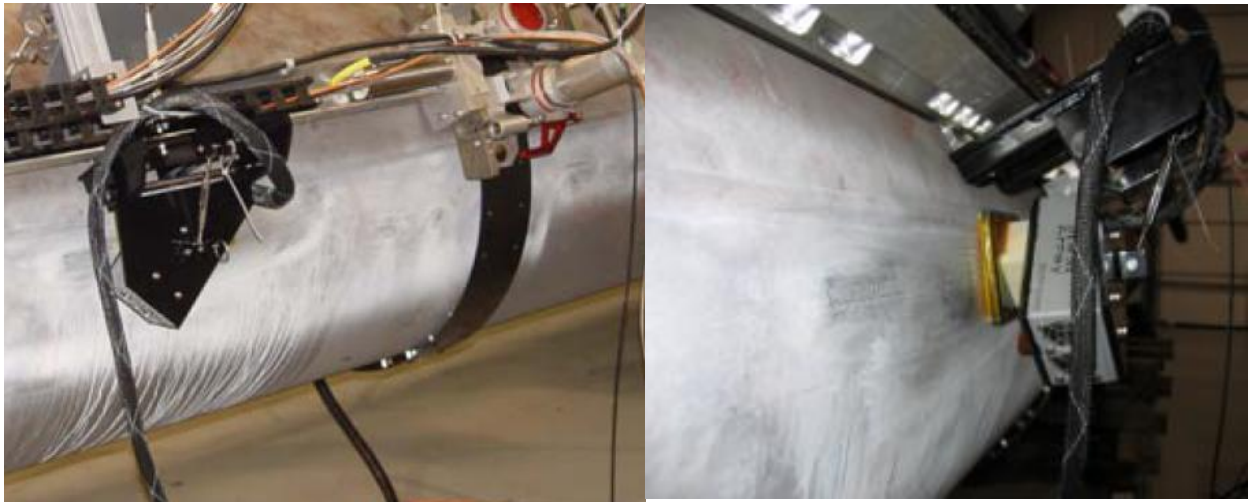


Figure 3: MWM-Array scanning to map surface SCC cracks. A crack map for pipe 10A is shown with the crack centreline tracking

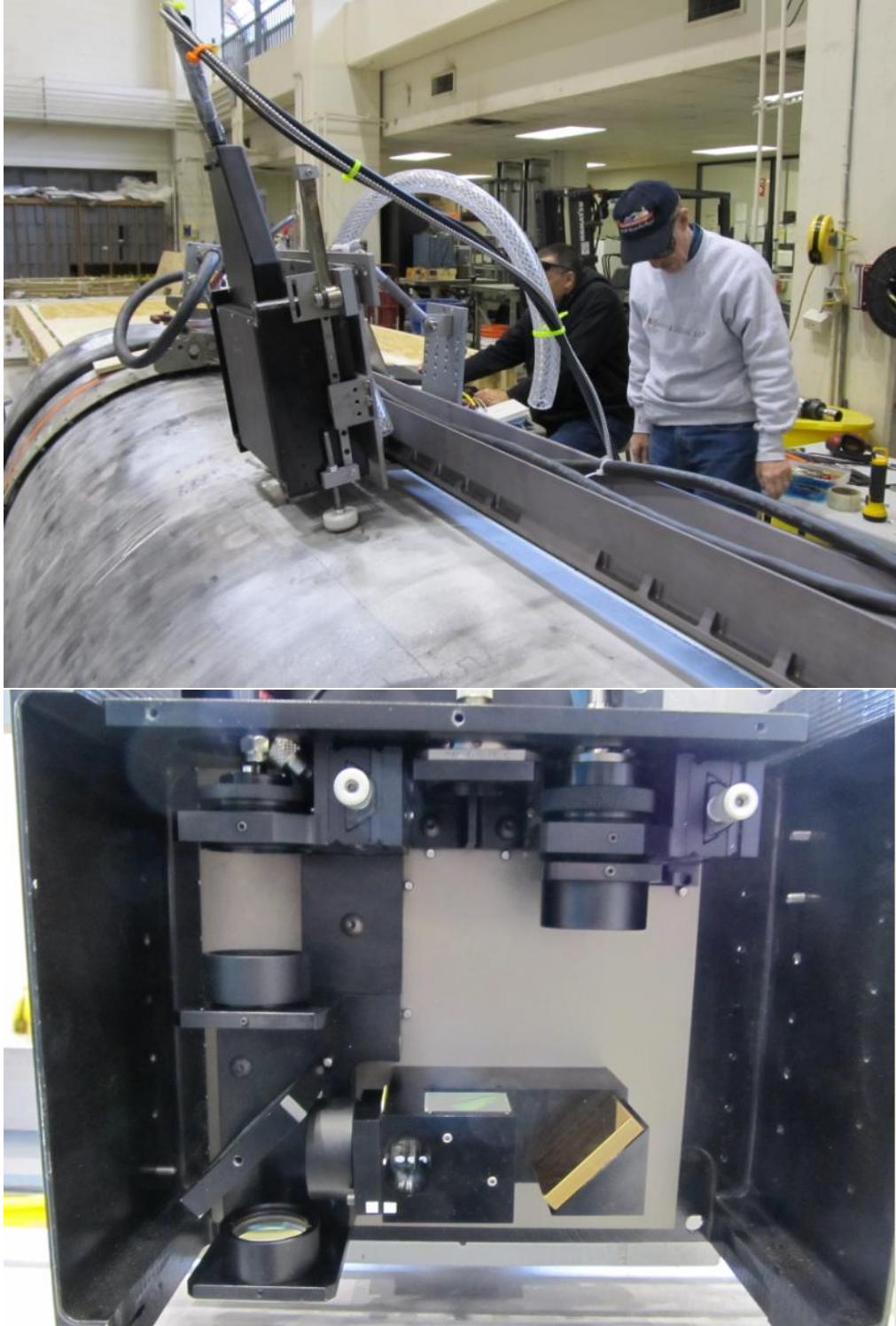


Figure 4: Photographs of the improved inspection head and fiber optic cable bundles. The inspection head travels axially along the lead screw rail shown and is driven circumferentially by actuator motors clamped to bands at each end of the lead screw rail.

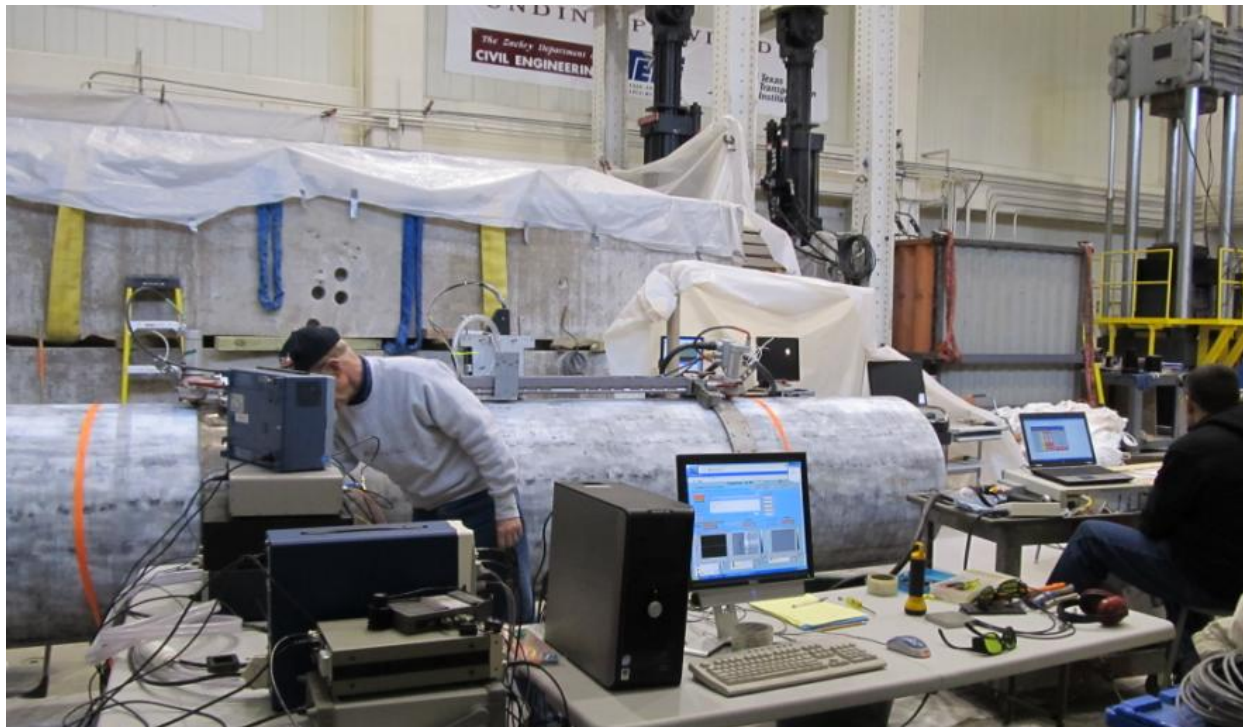
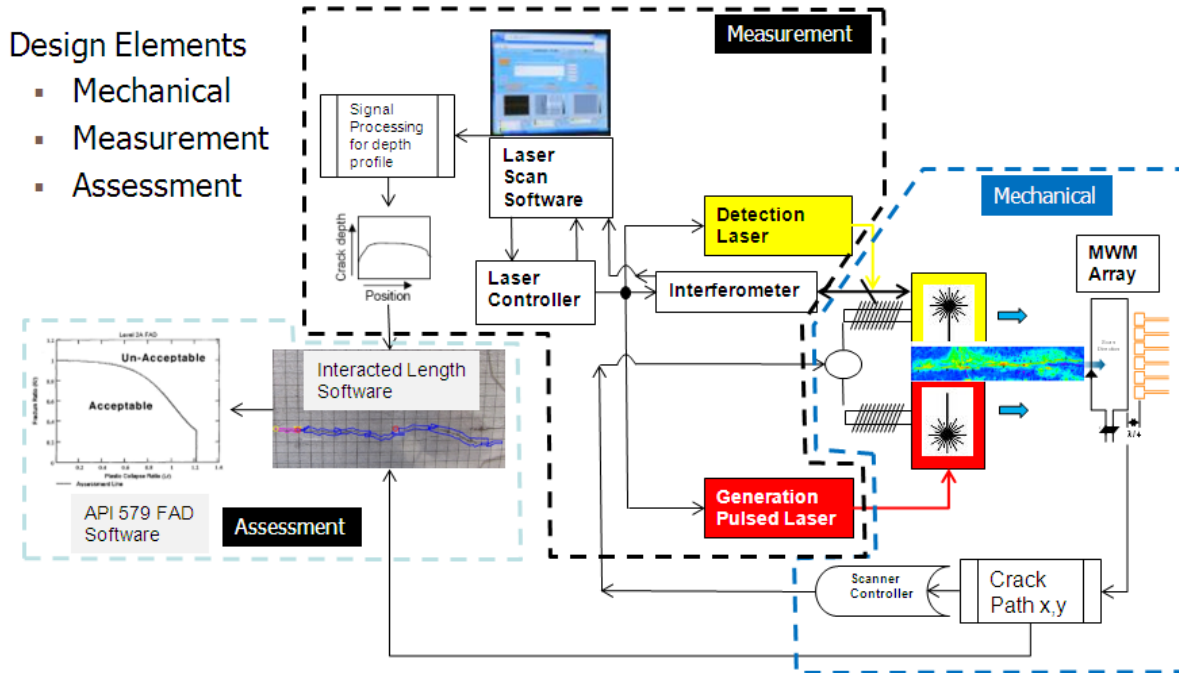


Figure 5: Functional illustration of the integrated tool process including the mechanical, signal analysis and integrity assessment elements. A photograph of the integrated tool set up at the field SCC trials is also shown. The scanner rail with laser measurement head is shown mounted on pipe with the signal analysis and Laser Scan™ software shown in the foreground. The hydrostatic test cell is shown in the background.



Figure 6: Photographs of typical configuration prepared for the hydrostatic pressure-to-failure test sample pipes and their arrangement within the pressure test cell at Texas A&M University Structural Engineering Laboratory.

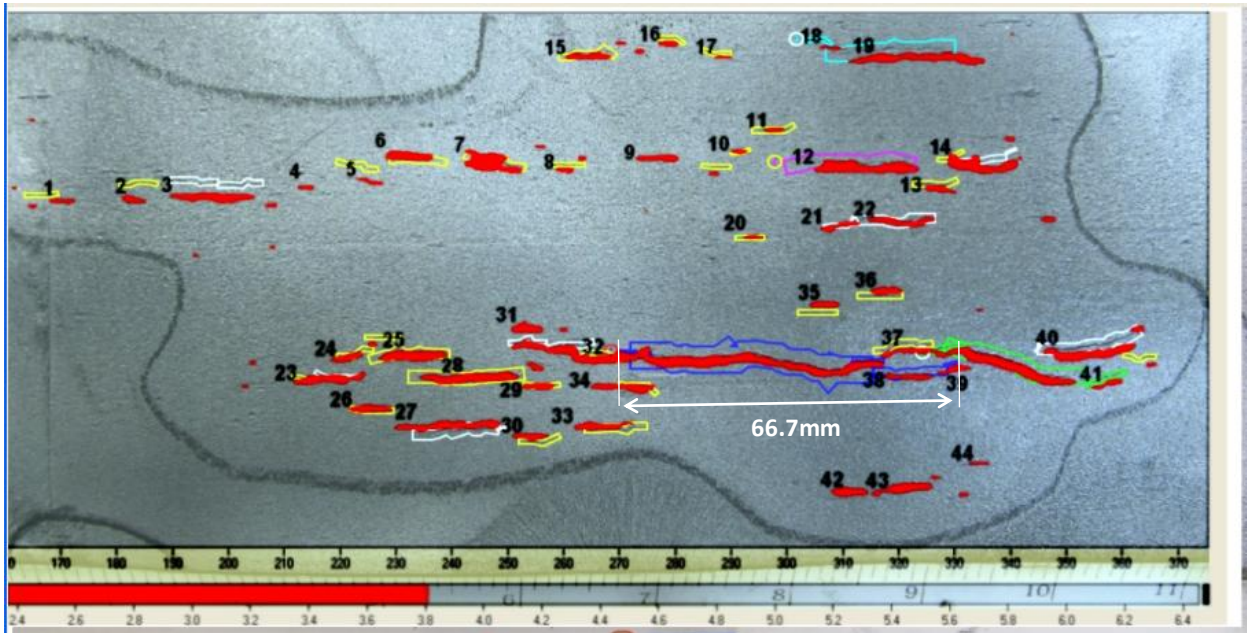


Figure 7: MWM-Array crack map from pipe #4 with NACE/CEPA interaction criterion applied measuring a maximum crack length of 66.7 mm. These measurements combined with depth screening by PA ultrasonic were evaluated by API 579 FAD to identify the most significant cracks within the colony for sizing by LToFD.

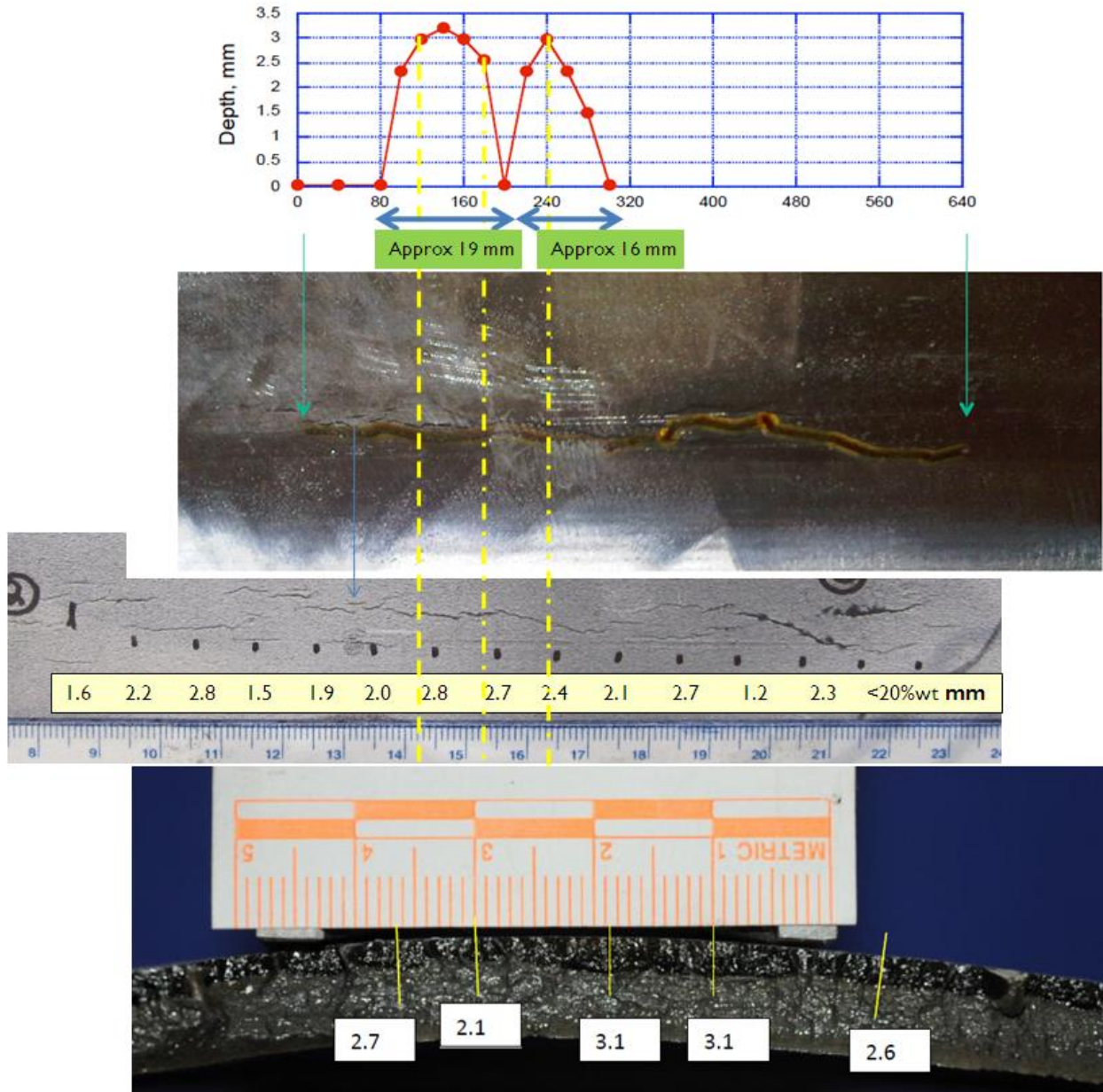


Figure 8: Results of LToFD depth sizing performed on target crack from Pipe # 4 showing good agreement between predicted depth and actual SCC depth determined from fractures surfaces obtained after hydrostatic test to failure.

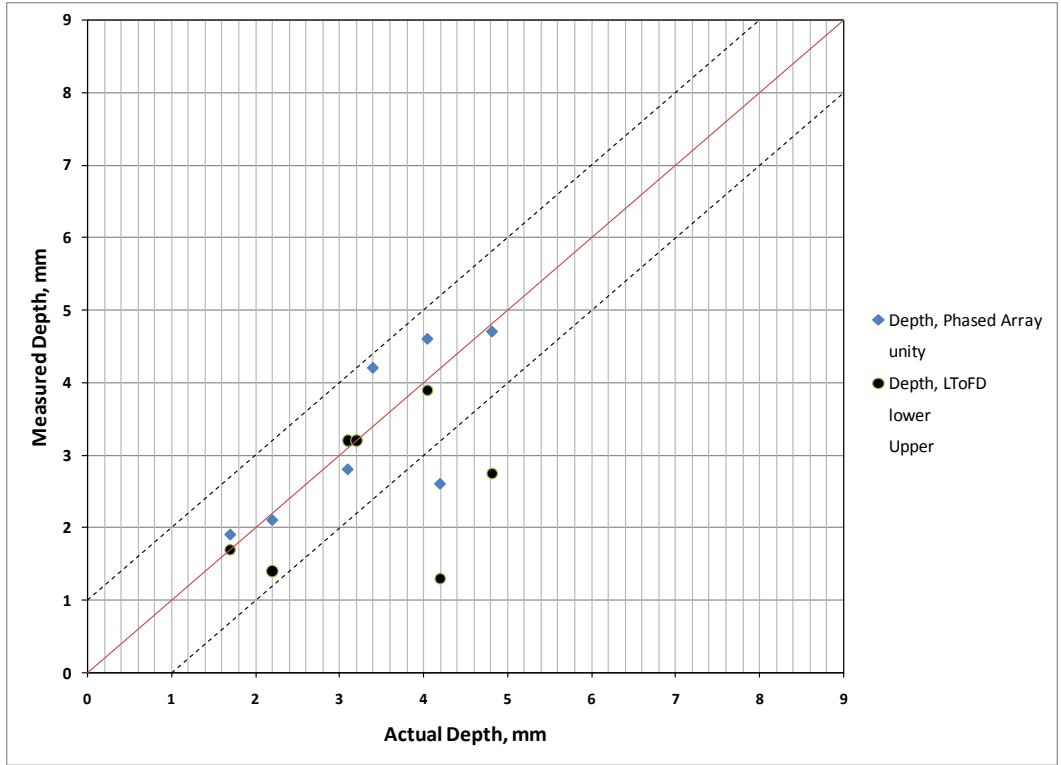


Figure 9: Crack depth unity plot comparing NDE measurements with actual crack depths measured from fracture surfaces.

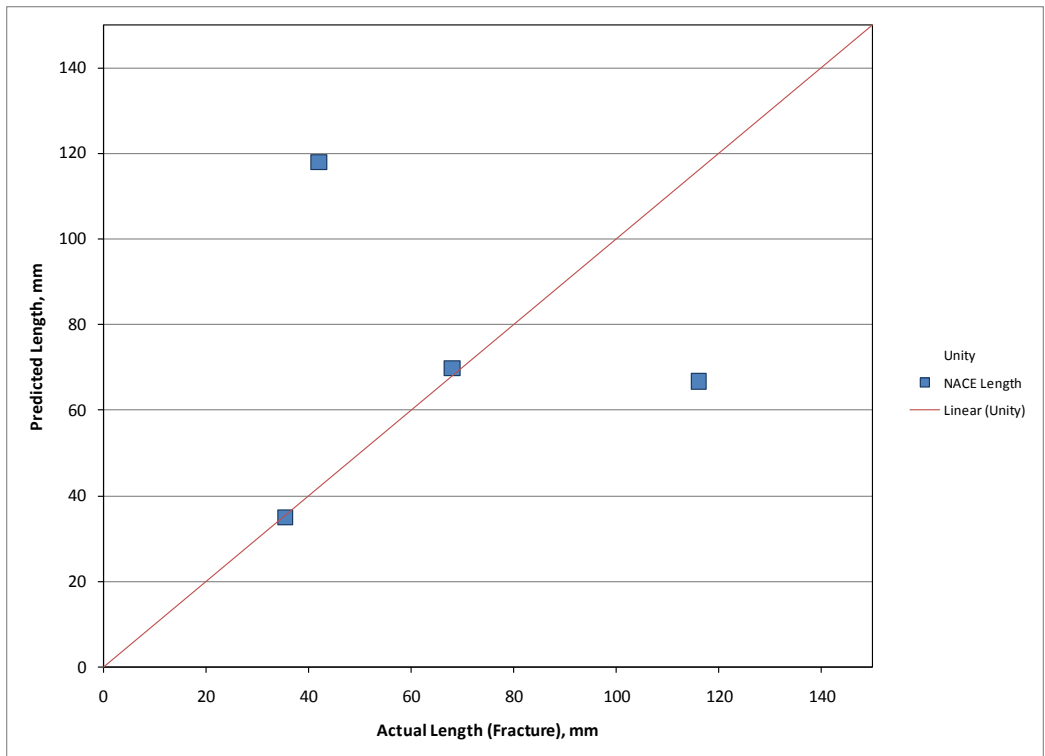


Figure 10: Comparison of actual interacted crack length from fracture surfaces with predicted maximum interacted length from NACE criterion.

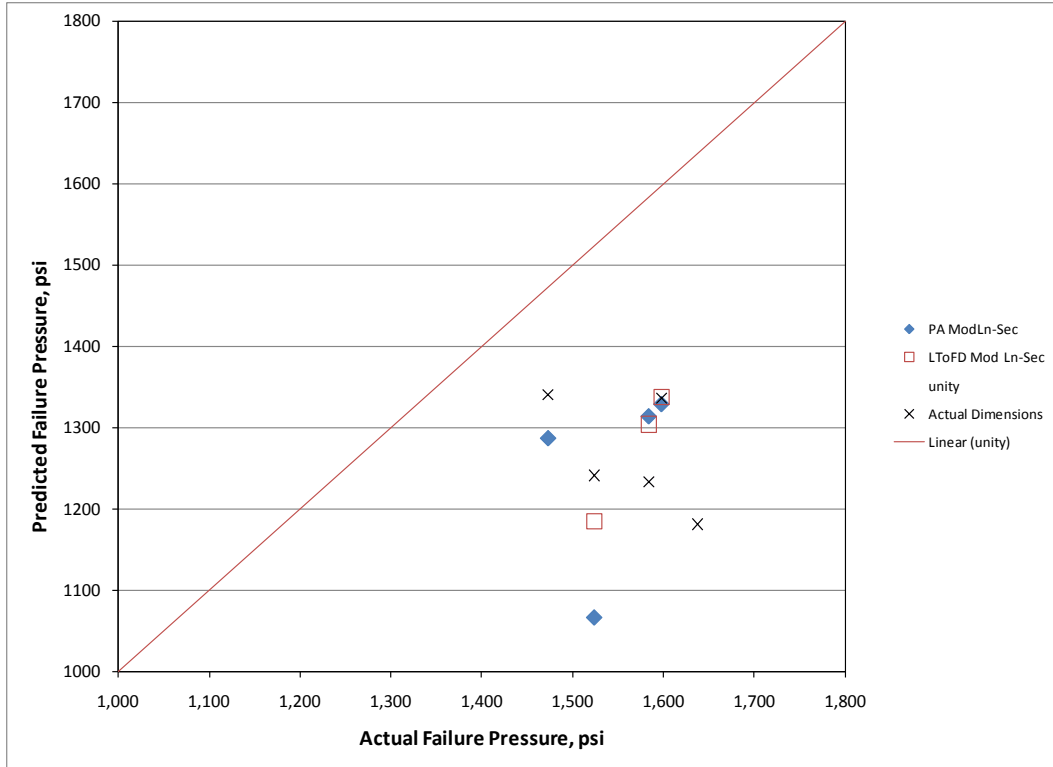


Figure 11: Failure pressure unity plot, NG-18 Mod Ln-Sec compared with actual hydrostatic test failure pressures.

Pipe #	Size		Pressure		Failure % SMYS	Comment	NDE Summary
	OD	Wall	psi	kPa			
2	36	0.374	1,417	9,770	124%	Ruptured	MPI, Toe Crack, SCC
3	36	0.374	1,391	9,590	121%	Ruptured	MPI, Toe Crack, SCC
4	34	0.385	1,584	10,922	138%	Ruptured	MPI,PA,LToFD, SCC
5	34	0.385	1,473	10,159	128%	Ruptured	MPI,PA,SCC
6 ‡	34	0.385	1,100	7,585	96%	Notched + Fatigued Ruptured	MPI,PA, SCC (<20%)
7 ‡	34	0.385	1,609	11,094	140%	Pipe bulged, did not burst.	MPI,PA, SCC (<20%)
8 ‡	34	0.385	909	6,268	79%	Notched + Fatigued Ruptured	MPI,PA, SCC (<20%)
9	36	0.374	No Test				MPI,PA,Toe Crack
12	34	0.385	No Test			Shallow crack depth	MPI,PA, SCC (<20%)
14	34	0.385	No Test			Shallow crack depth	MPI,PA,SCC
10A	36	0.374	1,524	10,508	133%	Ruptured	MPI,PA,LToFD,SCC
10B-1	36	0.374	1,638	11,294	143%	Leaked off-target location	MPI,PA,LToFD,SCC
10B-3*	36	0.374				Leaked off-target location	MPI,PA,LToFD,SCC
11A	36	0.374	1,454	10,026	127%	Ruptured	MPI,PA, Toe Crack
11B	36	0.374	1,643	11,329	143%	Rupture initiated at other location on seam weld	MPI,PA, Toe Crack
13-A*	34	0.385				Leaked at loc 13-C	MPI,PA,LToFD, SCC
13-B*	34	0.385				Leaked at loc 13-C	MPI,PA,LToFD, SCC
13-C	34	0.385	1,598	11,018	139%	Leaked at same location	MPI,PA,LToFD,SCC

Table 1: Hydrostatic pressure test-to-failure summary.

Notes: * - Non-target SCC indications did not fail but provided sizing data

‡ - Burst Validation for Category 0 and 1 insignificant SCC

Grey Shaded- Target SCC locations identified and hydrostatic pressure test

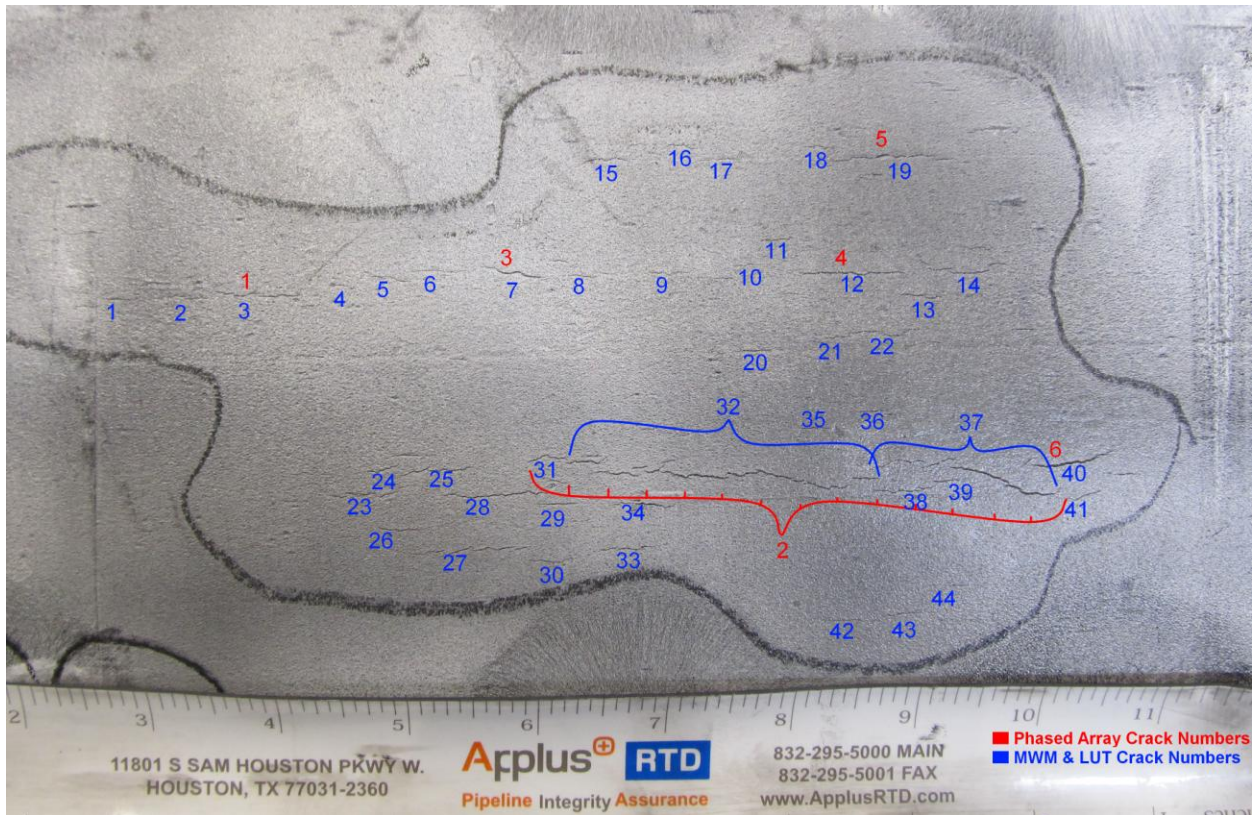
Annex A- Test Data

This annex contains detailed test data, both NDE and pressure-to-failure test for the five pipes with significant SCC determined by screening (MWM-Array, full 360 MPI, PA ultrasonic and API 579 FAD assessment). The highest likelihood crack feature within the SCC colonies was identified. Four of the five pipes were subjected to LToFD measurement of crack depth for the most significant SCC crack. One pipe was subjected to pressure test to failure as to validate the screening approach without LToFD. Data from the following pipes are contained within this Annex:

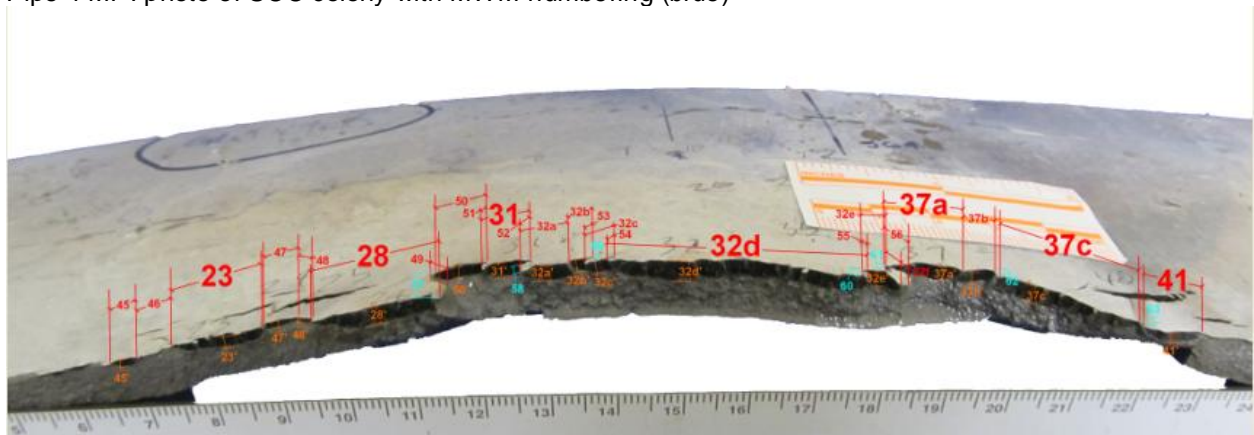
Pipe 4
Pipe 5- Control
Pipe 10A
Pipe 10 B
Pipe 13

Pipe 4

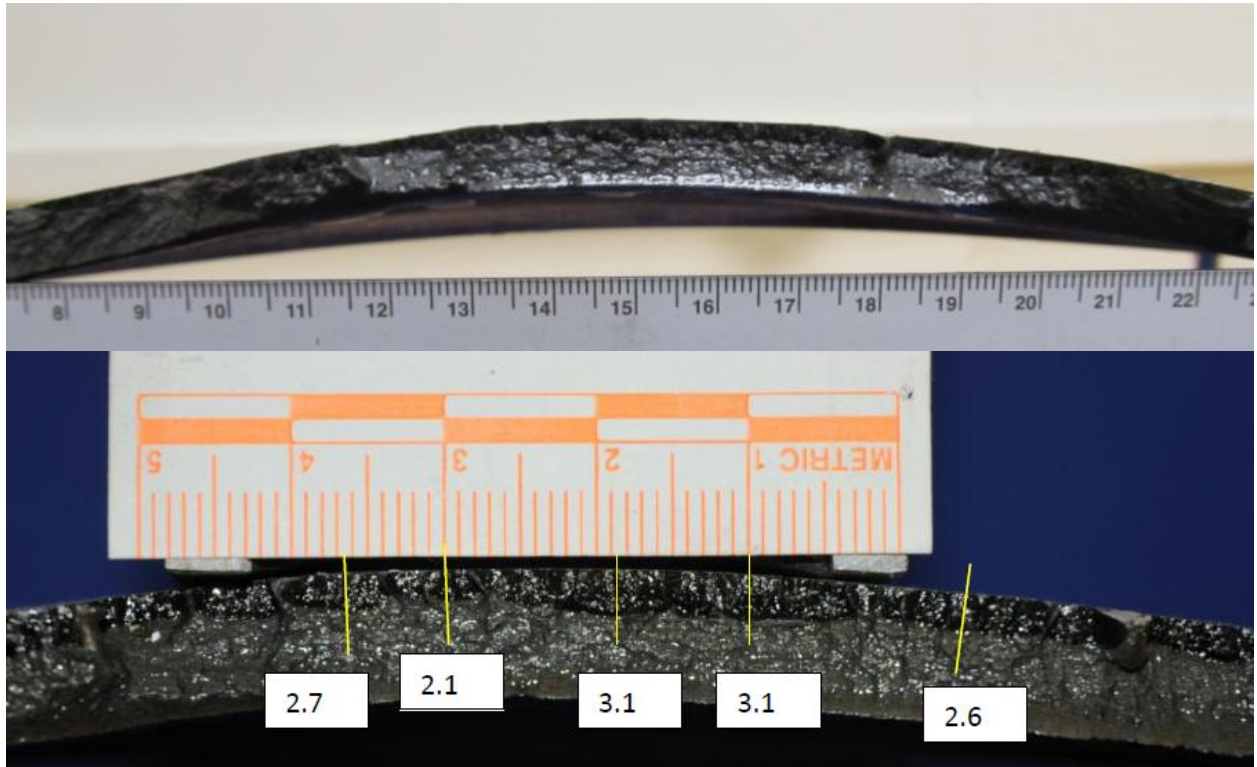
Numbering		From MWM				From Phased Array UT	
MWM	PA	X* (mm)	Y* (mm)	Length (mm)	Width (mm)	Depth (mm)	Depth (in)
1		170.3	104.7	4.3	2.4		
2		183.2	105.0	4.1	2.0		
3	1	197.2	105.3	14.9	2.2	1.8	0.071
4		213.9	107.6	2.8	1.1		
5		225.2	108.9	5.3	2.0		
6		232.4	114.6	8.6	2.2		
7	3	247.5	112.3	10.6	3.3	0.0	0.000
8		260.2	111.4	3.3	1.5		
9		276.8	113.9	7.9	1.8		
10		291.7	115.6	2.9	1.1		
11		297.7	120.3	3.3	1.3		
12	4	314.3	112.1	18.9	2.6	1.3	0.051
13		327.5	107.2	5.5	2.0		
14		335.4	112.8	13.4	4.4		
15		264.2	136.8	7.9	1.5		
16		278.8	139.4	3.5	1.5		
17		288.4	136.5	3.5	1.1		
18		308.4	138.6	5.1	0.9		
19	5	323.2	136.1	24.8	2.4	1.6	0.063
20		294.0	96.7	3.3	1.3		
21		309.6	98.9	7.1	2.6		
22		320.8	100.0	12.2	2.2		
23		218.2	65.3	12.8	2.6		
24		221.3	70.2	5.7	2.2		
25		233.1	70.2	12.4	2.6		
26		225.5	58.5	8.3	1.8		
27		239.3	54.6	19.0	2.9		
28		243.0	65.4	17.6	3.1		
29		255.5	63.4	5.9	1.8		
30		254.3	52.1	6.7	1.8		
31	2	253.5	76.7	5.8	2.6	2.2	0.087
32	2	284.1	69.7	66.6	8.2	2.8	0.110
33		267.4	54.8	10.8	1.9		
34		270.7	63.0	11.6	2.5		
35		306.8	81.5	5.6	1.7		
36		317.9	84.5	5.8	1.7		
37	2	334.2	67.9	35.0	8.7	2.7	0.106
38	2	321.9	65.5	9.0	1.3	2.7	0.106
39		330.0	67.1	6.1	2.2		
40	6	354.2	71.0	16.8	4.3	2.1	0.083
41		357.2	64.0	6.1	2.5		
42		311.3	40.1	6.7	1.8		
43		320.7	40.6	10.9	3.1		
44		334.4	46.4	4.1	0.8		



Pipe 4-MPI photo of SCC colony with MWM numbering (blue)



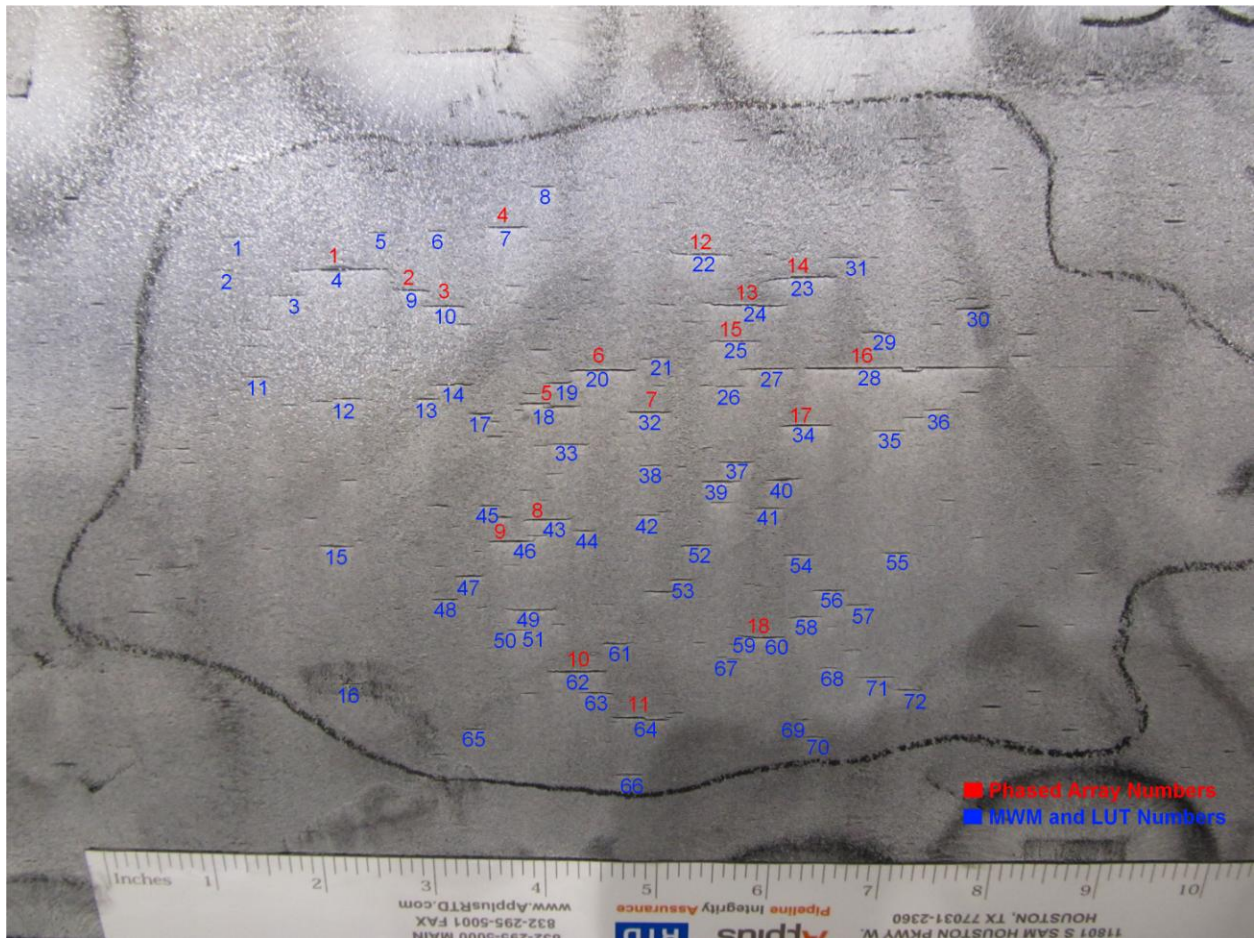
Pipe 4- Fracture surface after rupture at 1584 psi.



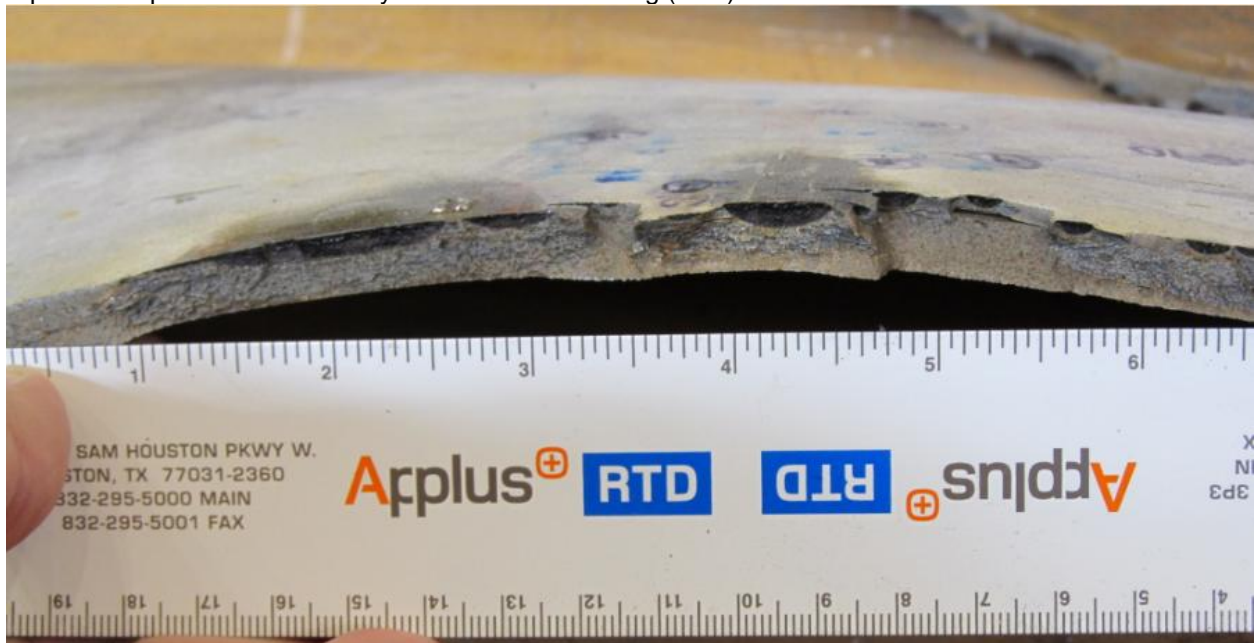
Pipe 4: Detailed measurements of interacted SCC crack profile after rupture at 1584 psi.

Pipe 5

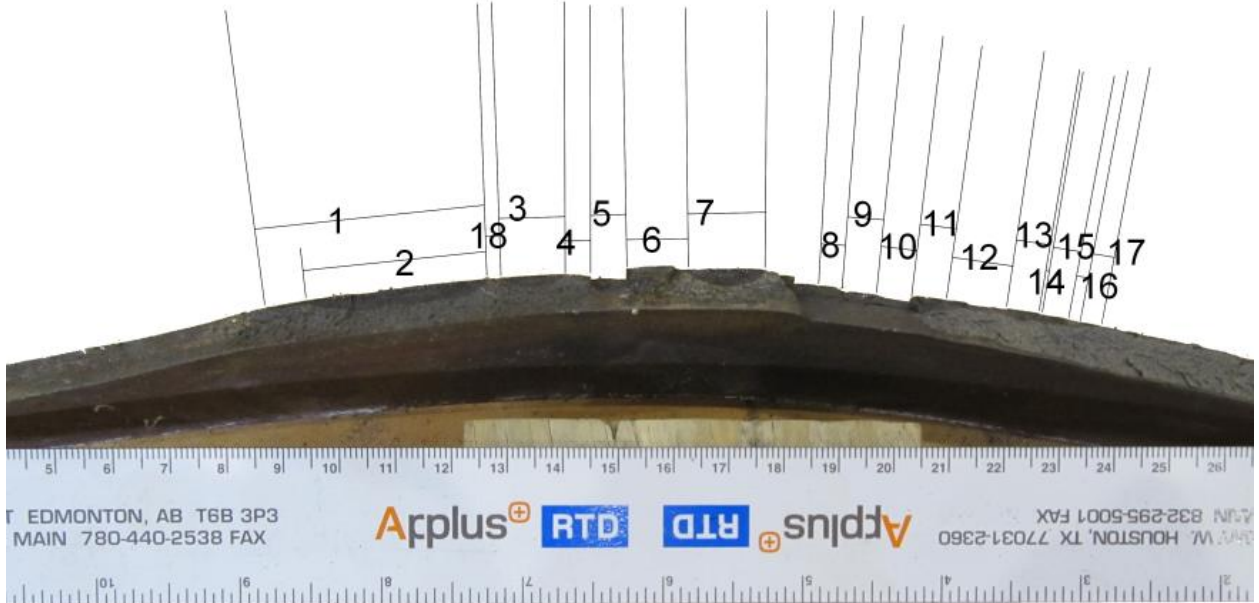
Numbering		From MWM				From Phased Array UT	
MWM	PA	X* (mm)	Y* (mm)	Length (mm)	Width (mm)	Depth (mm)	Depth (in)
1		87.3	166.2	3.3	1.2		
2		83.8	159.4	3.1	1.5		
3		96.8	154.0	5.8	2.0		
4	1	108.3	158.9	19.3	2.7	4.0	0.157
5		116.9	166.3	3.9	1.4		
6		129.1	166.1	2.6	1.7		
7	4	143.1	165.9	7.7	2.4	2.7	0.106
8		150.4	173.7	4.3	1.5		
9	2	123.5	154.4	6.3	1.8	2.7	0.106
10	3	128.1	148.7	8.3	2.3	2.9	0.114
11		89.6	135.2	3.0	1.8		
12		105.1	130.0	9.1	2.1		
13		123.9	130.0	5.7	2.6		
14		129.3	132.5	7.8	1.7		
15		104.3	97.5	6.4	1.8		
16		104.6	61.8	4.7	2.1		
17		135.7	126.5	4.3	1.8		
18	5	149.0	129.0	12.4	4.9	2.6	0.102
19		151.3	132.5	5.2	2.0		
20	6	160.1	134.8	12.2	2.0	4.1	0.161
21		170.4	137.4	4.3	1.4		
22	12	180.3	1159.9	10.2	2.0	3.5	0.138
23	14	201.7	155.3	14.1	2.0	4.0	0.157
24	13	187.4	147.7	16.0	2.9	4.2	0.165
25	15	185.4	140.4	9.8	2.0	0.0	0.000
26		184.8	131.5	4.4	1.4		
27		191.6	134.8	9.8	1.7		
28	16	218.9	133.9	37.9	2.9	4.2	0.165
29		214.4	141.4	5.9	2.3		
30		234.3	145.9	4.9	2.3		
31		210.7	159.5	4.9	1.2		
32	7	169.2	126.4	7.3	1.8	2.9	0.114
33		152.0	120.0	9.7	2.1		
34	17	200.2	123.0	9.5	2.0	2.3	0.091
35		217.8	121.4	6.9	1.7		
36		225.0	13.9	8.2	3.2		
37		185.9	115.8	5.8	2.3		
38		169.3	115.4	3.2	1.5		
39		183.5	110.1	7.7	1.8		
40		196.9	111.4	7.3	3.8		
41		193.8	104.8	5.5	1.8		
42		167.8	103.1	5.2	1.8		
43	8	146.7	102.4	8.9	2.1	2.7	0.106
44		154.1	100.0	3.8	2.0		
45		136.0	105.4	3.3	1.5		
46	9	141.4	98.4	10.5	3.3	2.1	0.083
47		131.0	90.8	4.3	1.5		
48		126.0	85.8	4.6	1.5		
49		142.7	83.1	9.4	2.0		
50		140.3	78.6	3.6	1.8		
51		141.4	74.4	4.7	2.4		
52		178.2	96.9	5.9	1.8		
53		174.3	89.4	4.8	1.5		
54		199.6	95.7	5.7	2.0		
55		219.5	97.2	4.6	1.8		
56		205.9	89.1	6.4	2.1		
57		211.8	85.9	3.7	1.7		
58		200.8	82.7	7.0	2.4		
59	18	191.8	76.6	9.5	2.9	3.4	0.134
60		191.2	72.3	9.7	1.8		
61		160.2	71.5	5.5	1.8		
62	10	152.4	64.7	11.1	2.6	2.8	0.110
63		155.6	60.4	6.5	2.1		
64	11	165.6	54.4	15.6	3.5	2.9	0.114
65		130.3	50.8	3.6	1.8		
66		162.1	40.5	6.0	1.8		
67		183.9	67.7	5.1	2.1		



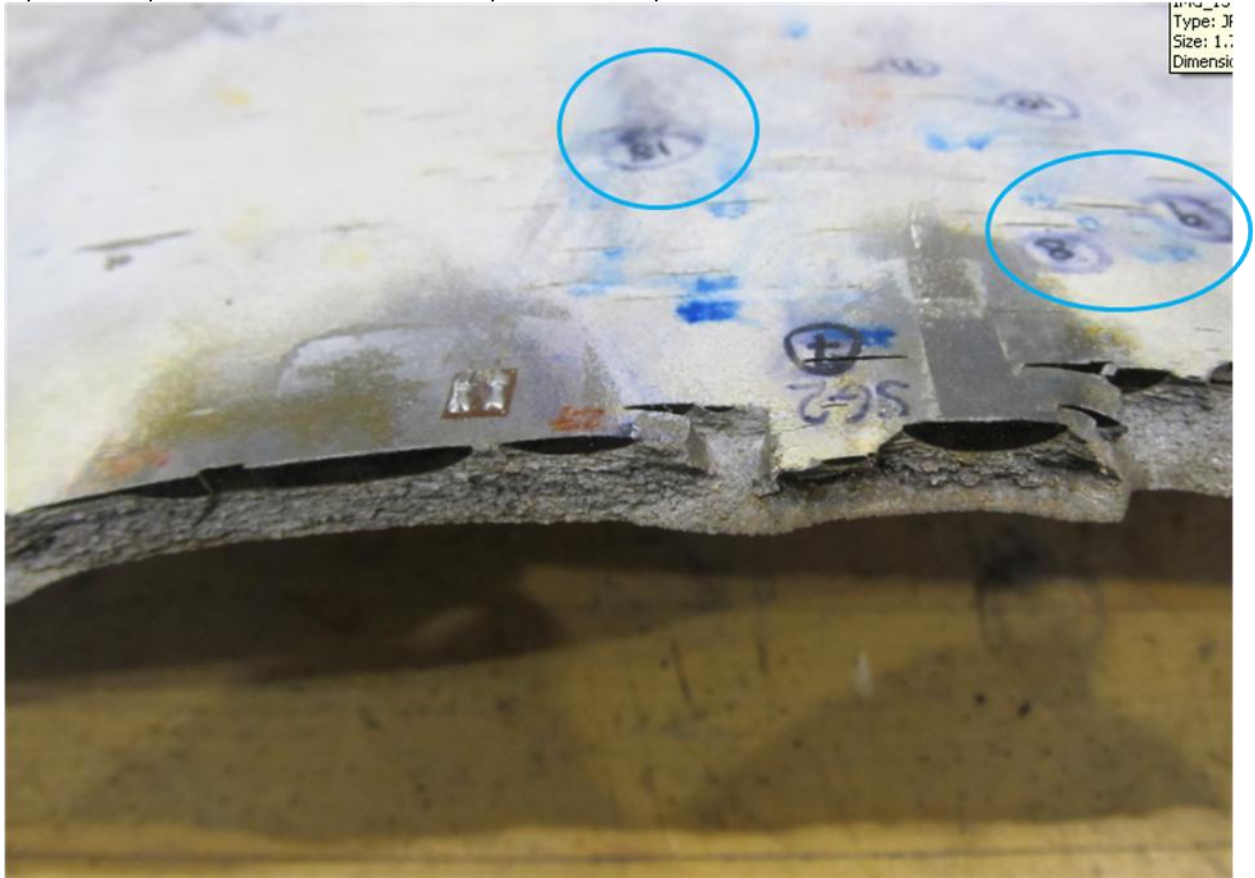
Pipe 5: MPI photo of SCC colony with MWM numbering (blue)



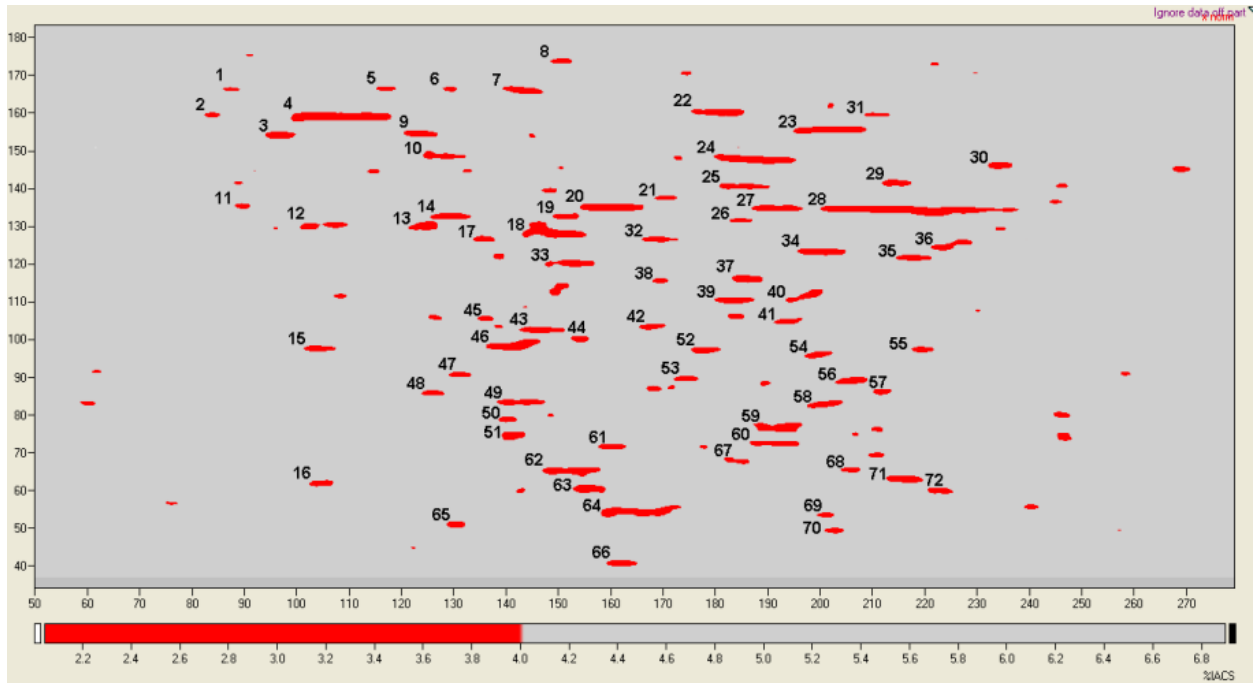
Pipe 5: Fracture surface after rupture at 1473 psi.



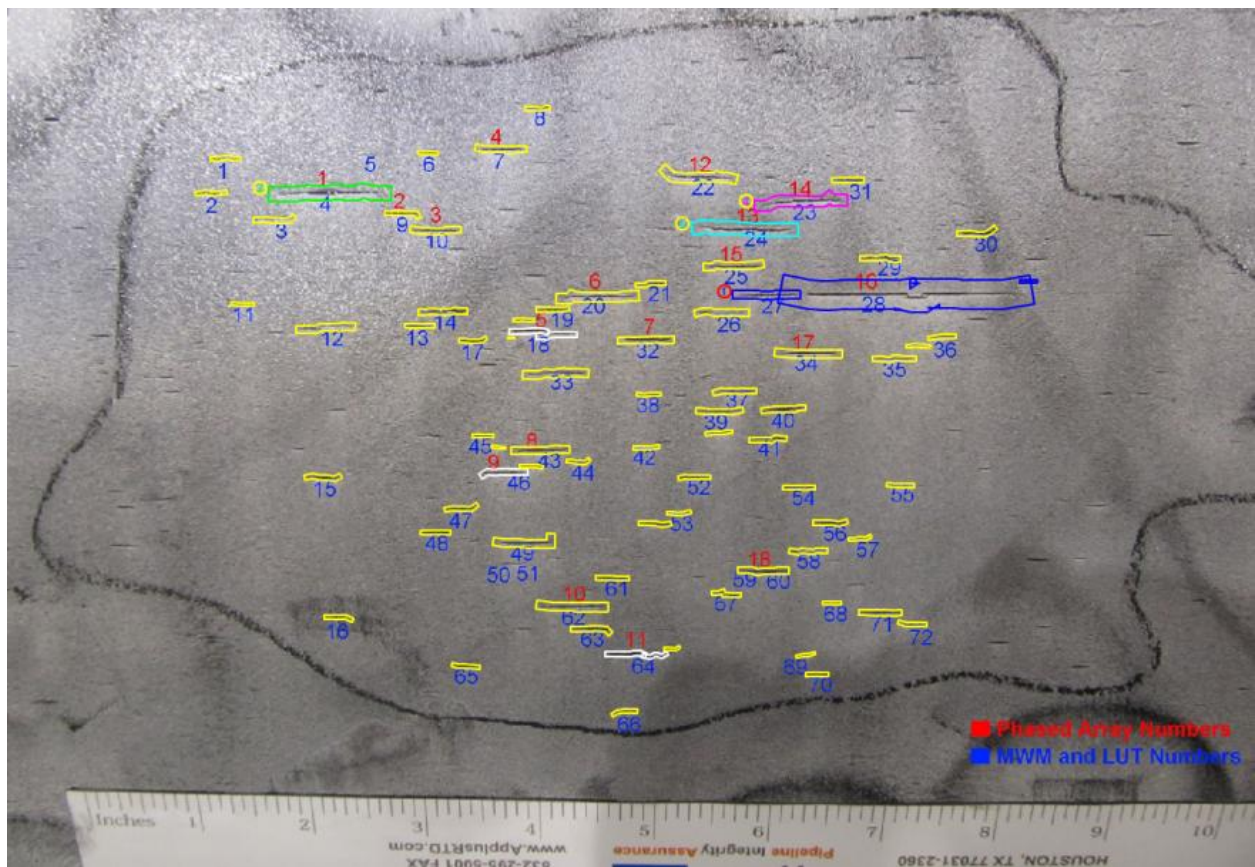
Pipe 5: Complete fracture surface after rupture at 1473 psi



Pipe 5: Fracture surface showing reference markers for orientation with the red phased array crack markers.



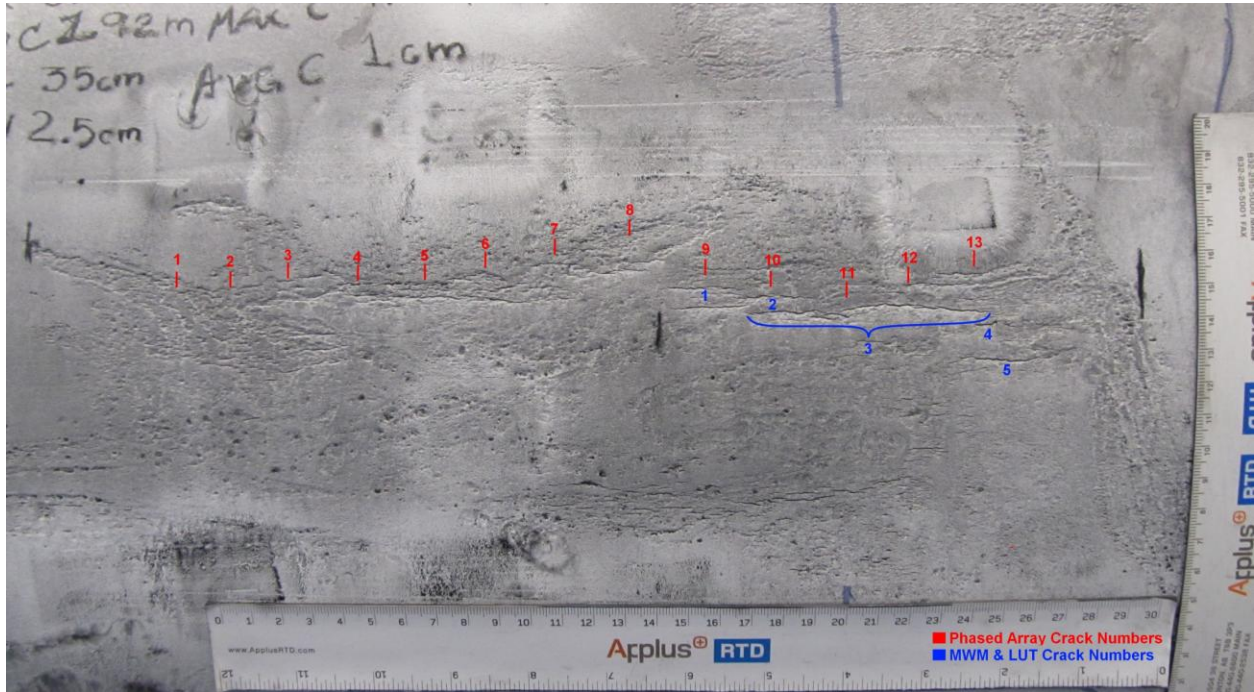
Pipe 5: MWM-array surface crack mapping



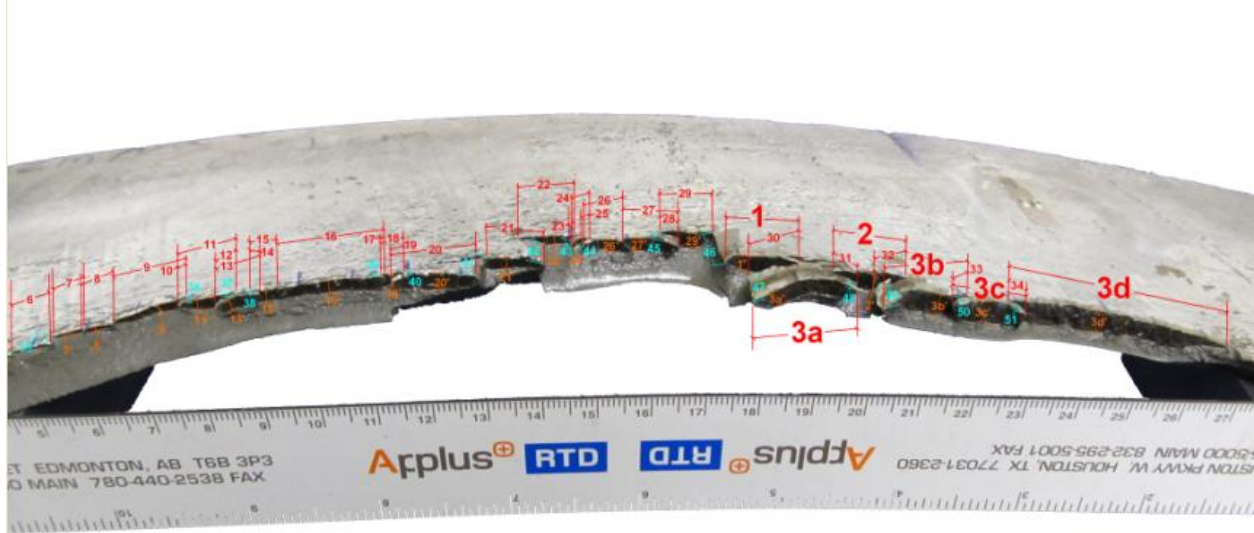
Pipe 5: NACE crack interaction program tracks overlain on MPI photograph

Pipe 10A

Numbering		From MWM				From Phased Array	
MWM	PA	X* (mm)	Y* (mm)	Length (mm)	Width (mm)	Depth (mm)	Depth (in)
1	9	267.8	104.1	19.2	4.5	3.3	0.131
2	10	284.7	102.4	19.0	3.3	3.4	0.135
3	13	314.0	97.4	63.2	7.8	4.7	0.186
4	13	352.7	61.9	6.3	2.9	4.7	0.186
5		354.7	80.6	21.0	4.8		
	1	#N/A	#N/A	#N/A	#N/A	2.3	0.092
	2	#N/A	#N/A	#N/A	#N/A	1.9	0.076
	3	#N/A	#N/A	#N/A	#N/A	2.7	0.108
	4	#N/A	#N/A	#N/A	#N/A	2.6	0.103
	5	#N/A	#N/A	#N/A	#N/A	3.5	0.137
	6	#N/A	#N/A	#N/A	#N/A	2.2	0.087
	7	#N/A	#N/A	#N/A	#N/A	2.6	0.101
	8	#N/A	#N/A	#N/A	#N/A	2.7	0.108



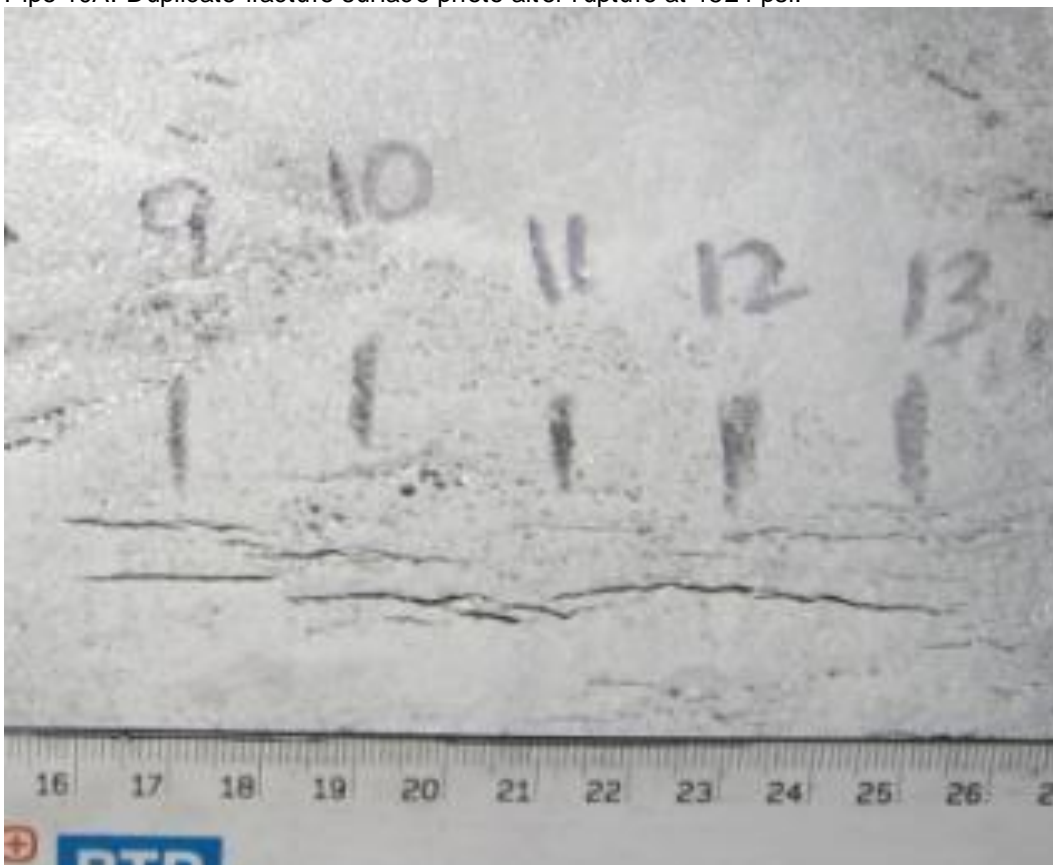
Pipe 10A: MPI photo of SCC colony with MWM numbering (blue)



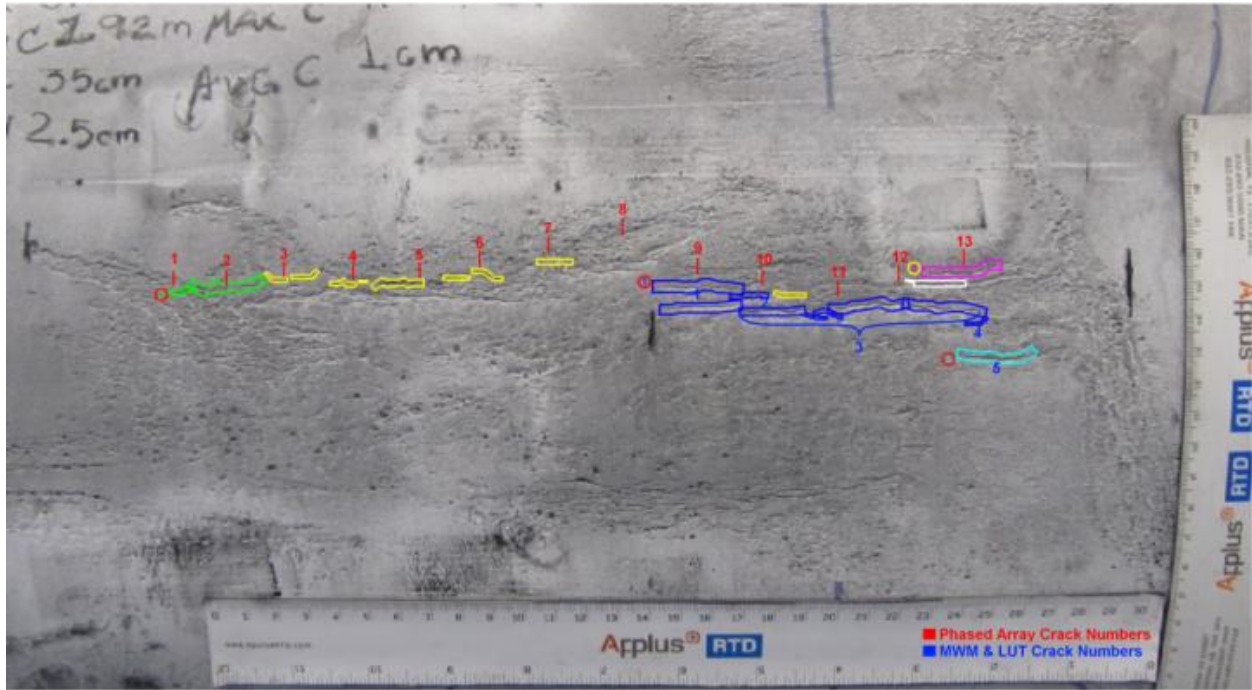
Pipe 10A: Complete fracture surface after rupture at 1524 psi



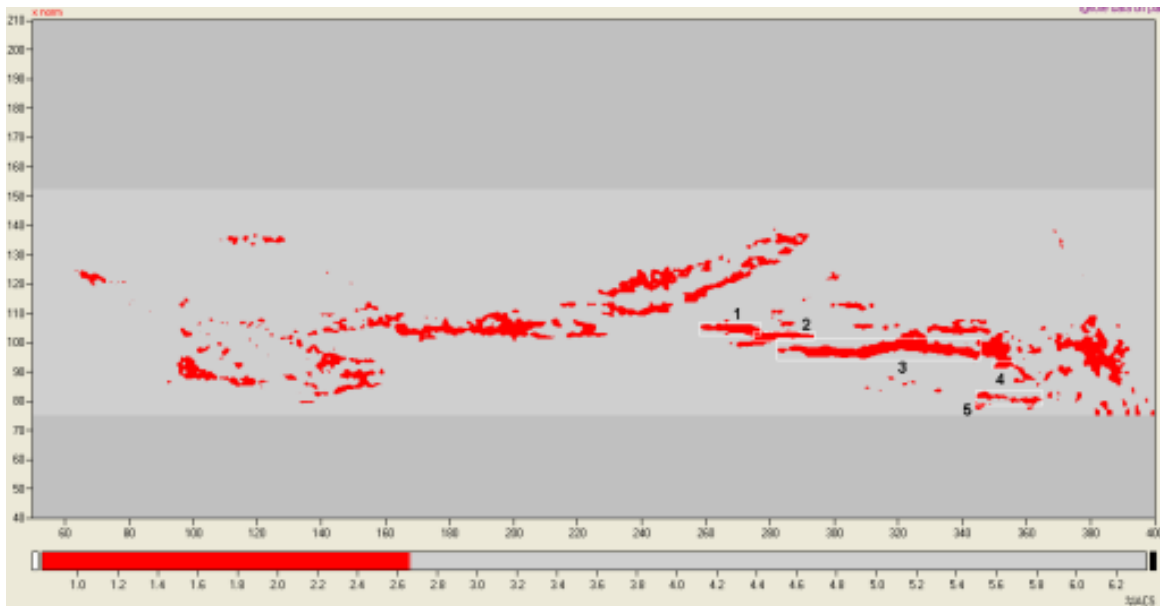
Pipe 10A: Duplicate fracture surface photo after rupture at 1524 psi.



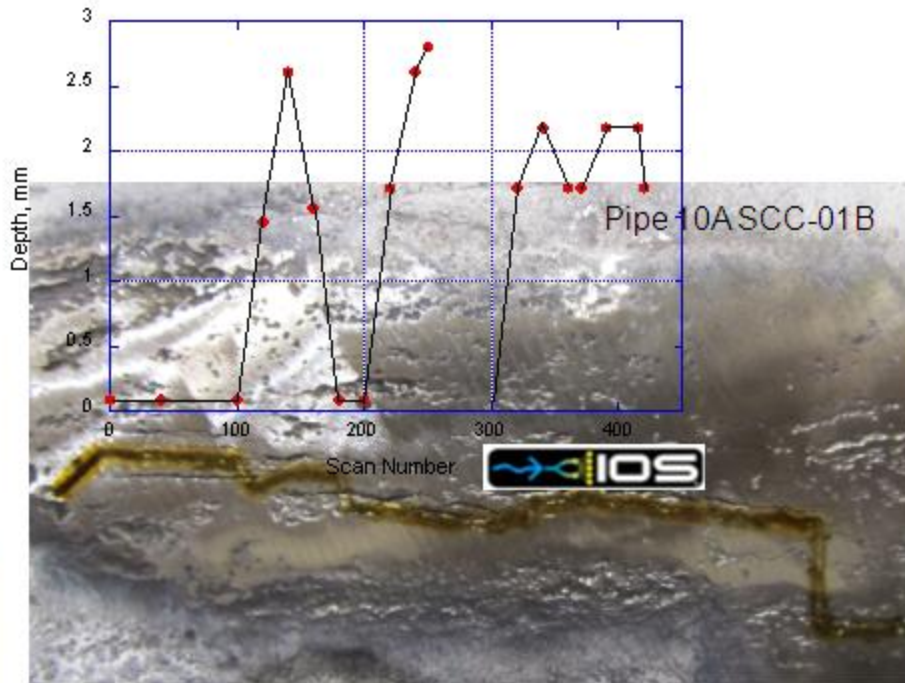
Pipe 10A: MPI Close-up view of crack MWM 3 with PA index marks



Pipe 10A: NACE crack interaction program tracks overlain on MPI photograph



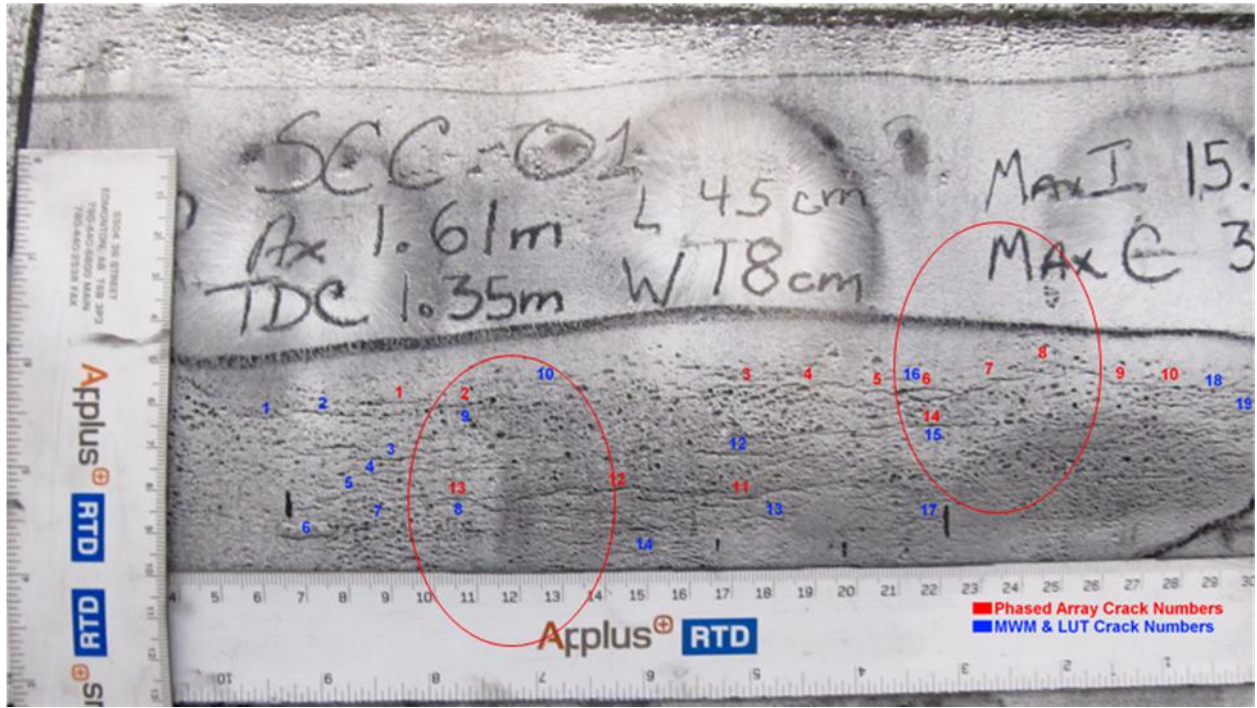
Pipe 10A: MWM-Array surface crack map showing MWM crack 3



Pipe 10A: Significant target crack in SCC colony (MWM 32) showing ablation track of generation laser with LToFD sizing overlain.

Pipe 10B

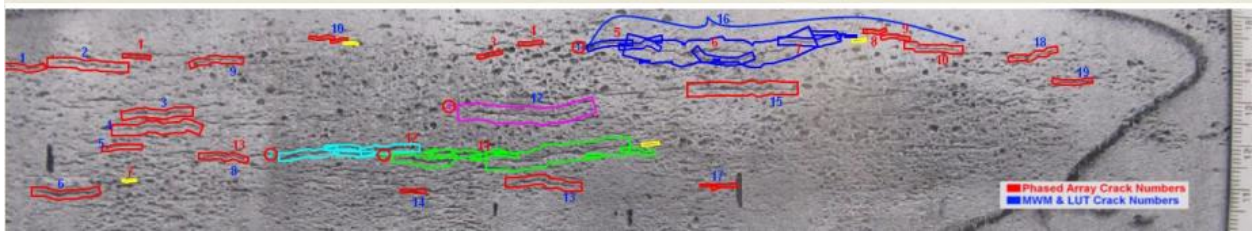
Numbering		From MWM				From Phased	
MWM	PA	X* (mm)	Y* (mm)	Length (mm)	Width (mm)	Depth (mm)	Depth (in)
1		43.2	77.1	14.3	3.4		
2		58.0	76.8	10.1	2.3		
3		69.8	71.4	31.0	4.8		
4		72.0	66.8	14.7	3.1		
5		68.5	63.3	16.1	6.1		
6		57.3	52.6	17.4	5.8		
7		70.8	57.7	10.5	4.9		
8	11	119.5	55.9	86.8	15.9	2.3	0.091
8	12	119.5	55.9	86.8	15.9	2.5	0.099
8	13	119.5	55.9	86.8	15.9	1.9	0.076
9	2	91.6	78.5	10.1	2.9	1.5	0.059
10		109.0	82.9	11.2	2.2		
11		99.3	41.2	14.0	4.6		
12		165.9	71.1	31.1	5.9		
13		175.7	64.0	23.6	4.8		
14		158.6	57.1	18.5	3.8		
15	14	197.6	78.2	27.3	5.8	1.9	0.074
16	3	207.5	86.8	82.6	10.9	1.8	0.072
16	4	207.5	86.8	82.6	10.9	4.8	0.189
16	5	207.5	86.8	82.6	10.9	1.8	0.069
16	6	207.5	86.8	82.6	10.9	2.1	0.083
16	7	207.5	86.8	82.6	10.9	1.7	0.065
16	8	207.5	86.8	82.6	10.9	1.7	0.067
16	9	207.5	86.8	82.6	10.9	2.5	0.097
16	10	207.5	86.8	82.6	10.9	1.5	0.059
17		197.4	56.6	9.7	2.9		
18		256.8	83.8	11.4	5.7		
19		263.9	80.3	7.7	3.2		
20		273.6	80.6	12.4	3.5		
21		282.7	82.4	5.2	2.9		
	1	#N/A	#N/A	#N/A	#N/A	2.7	0.106



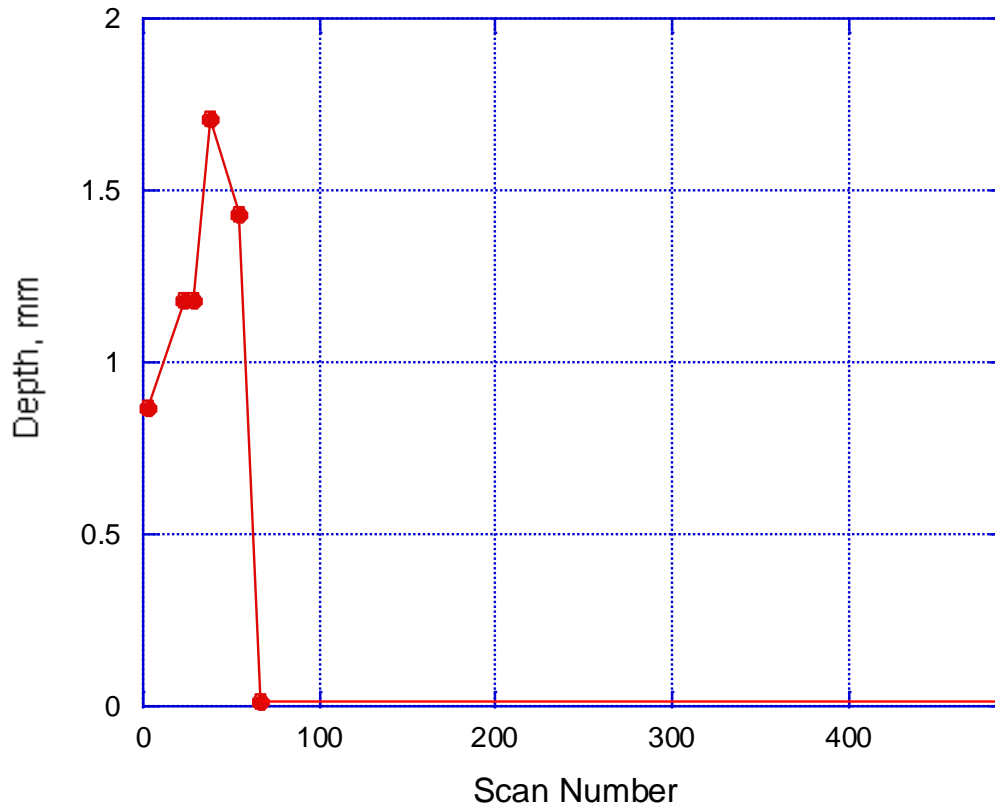
Pipe 10B: MPI photo of SCC colony with MWM numbering (blue), red circles indicate LToFD target locations



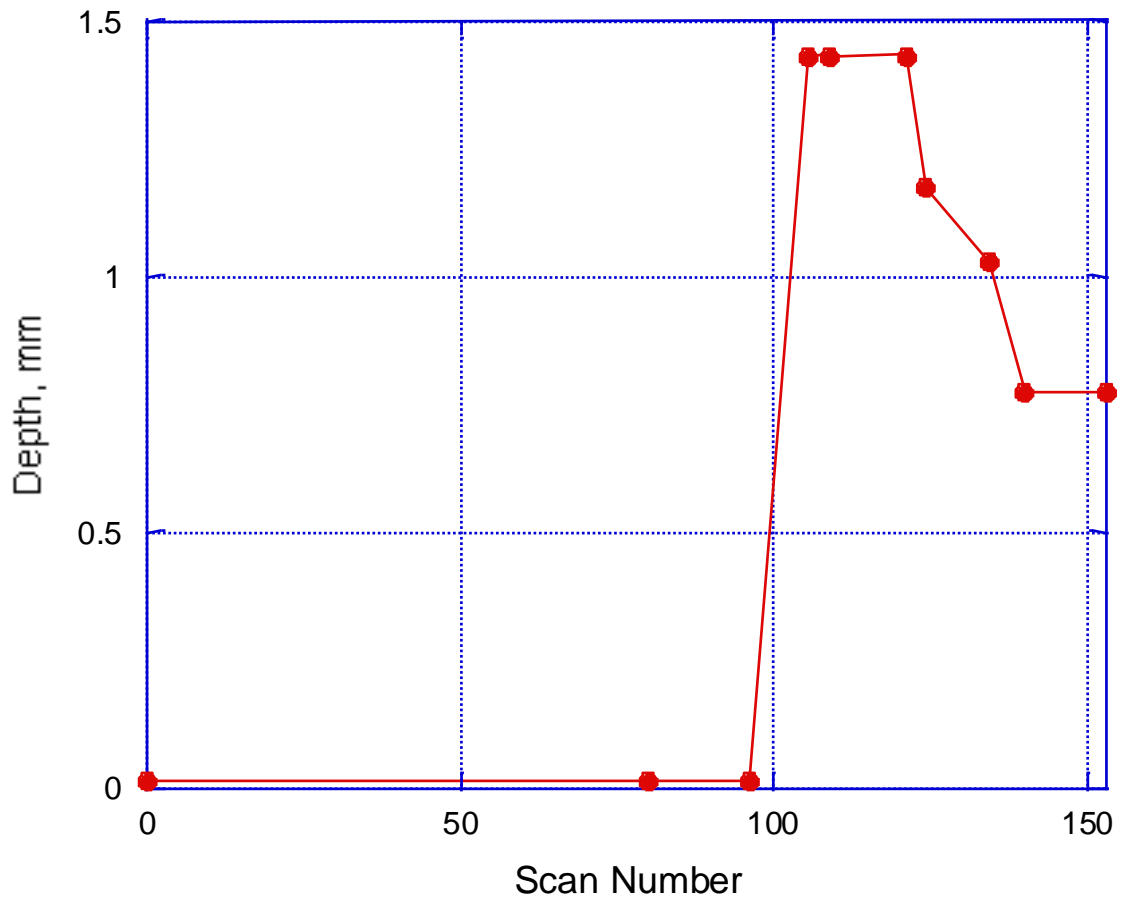
Pipe 10B: Target locations after leak at non-target location; 1638 psi



Pipe 10B: NACE crack interaction program tracks overlain on MPI photograph



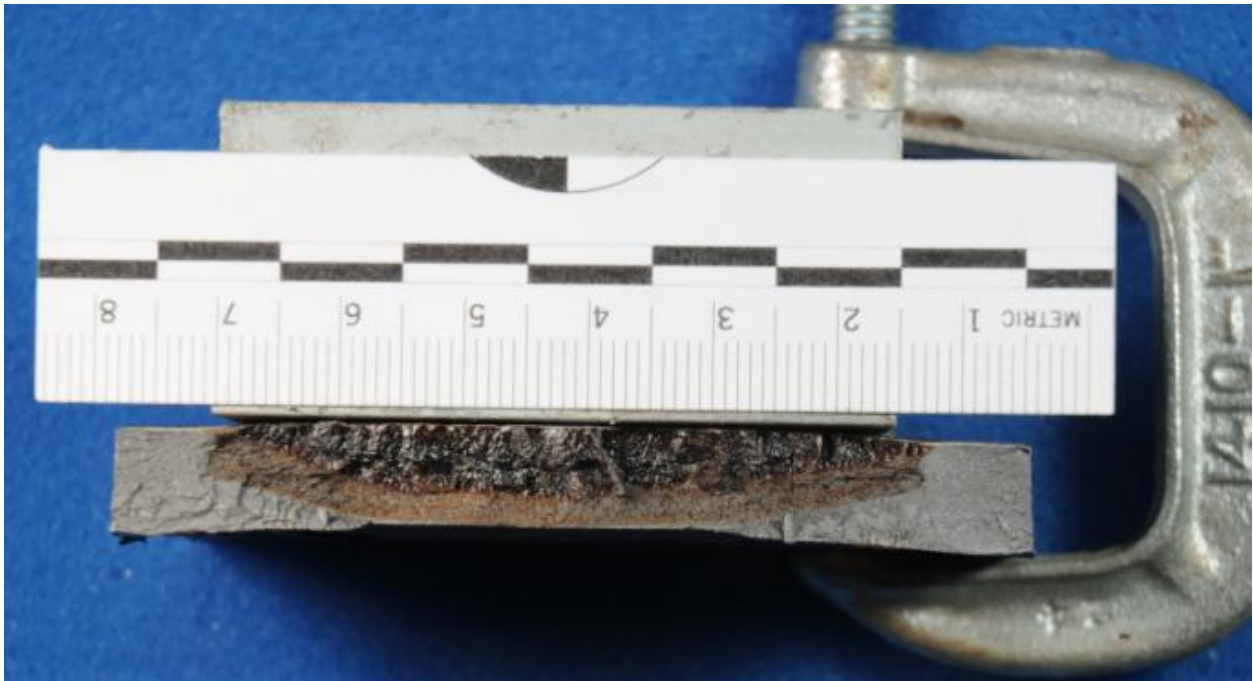
Pipe 10B: Depth sizing data for target MWM 8



Pipe 10B: Depth sizing data for target MWM 16 (PA 6,7,8)



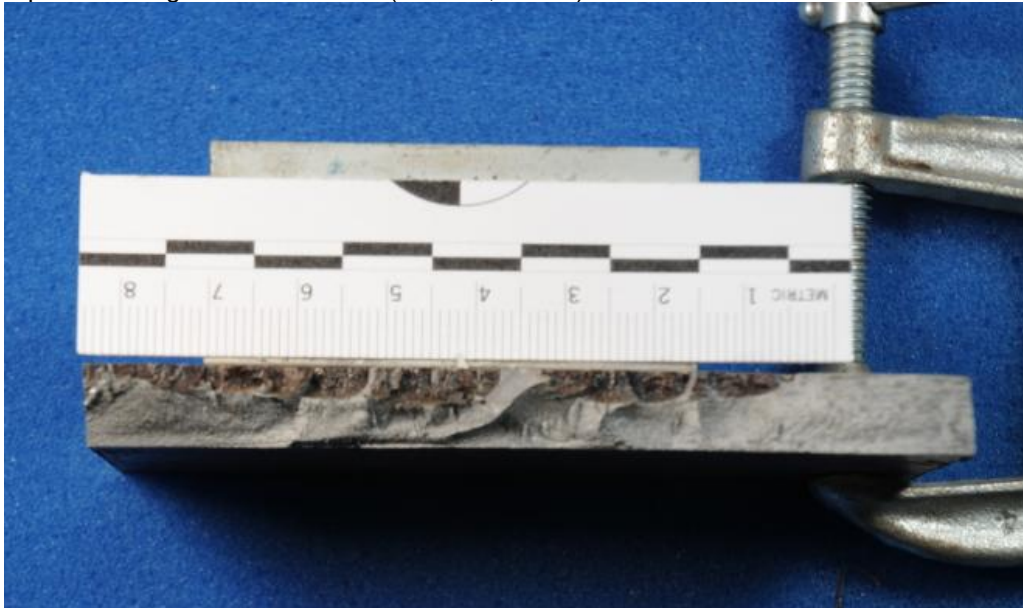
Pipe 10B: Pipe surface at non-target leak location



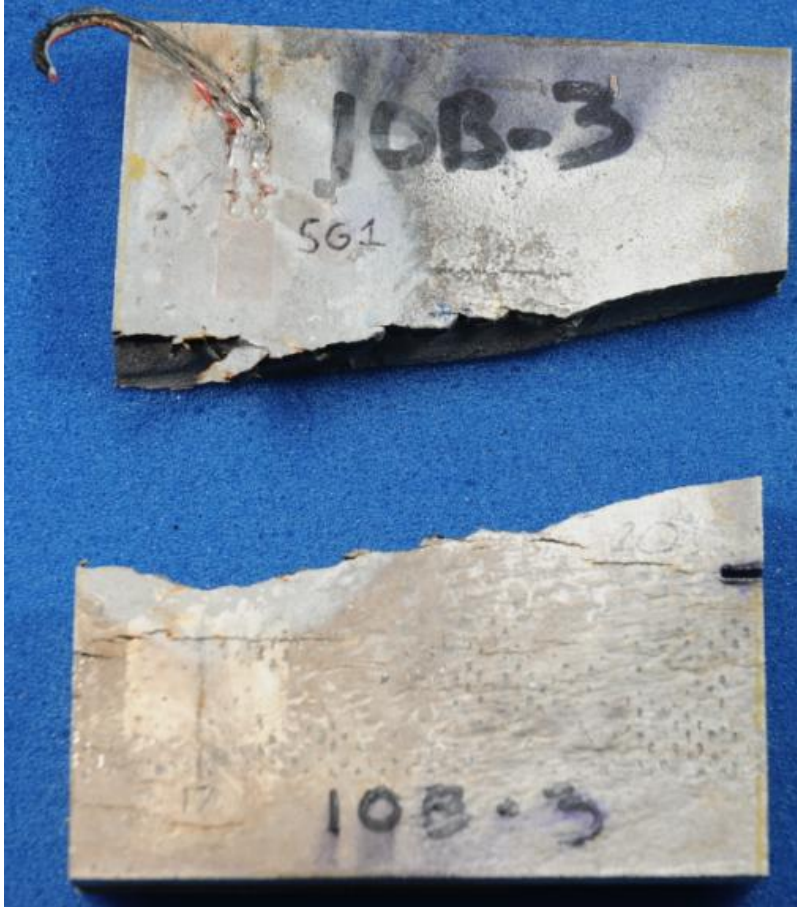
Pipe 10B: Non-target leak location at 1638 psi



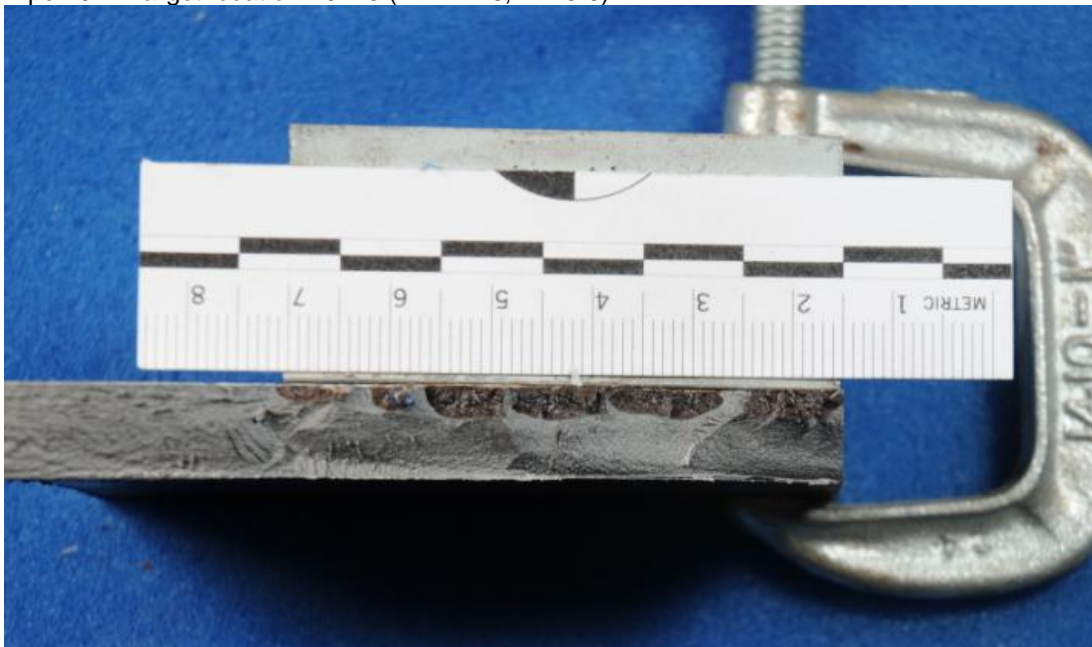
Pipe 10B: Target location 10B-1 (MWM 8, PA 12)



Pipe 10B: Target location 10B-1 Fracture surface, frozen by liquid nitrogen and broken after leak at off-target location.



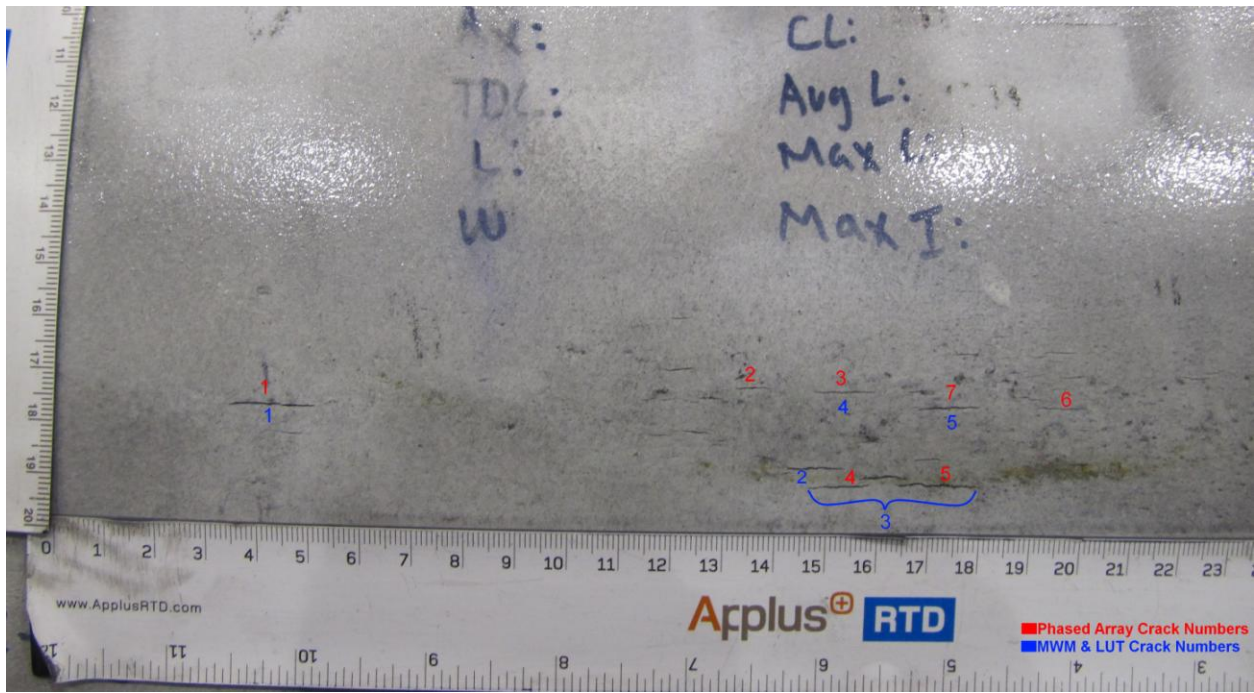
Pipe 10B: Target location 10B-3 (MWM 16, PA 3-9)



Pipe 10B: Target location 10B-3 fracture surface frozen by liquid nitrogen and broken after leak at off-target location.

Pipe 13

Numbering		From MWM				From Phased Array	
MWM	PA	X* (mm)	Y* (mm)	Length (mm)	Width (mm)	Depth (mm)	Depth (in)
1	1	59.3	62.5	14.4	1.6	2.6	0.103
2		157.2	48.0	10.1	2.1		
3	5	171.7	45.0	29.3	4.3	4.6	0.183
4	3	162.7	61.8	8.6	2.1	NA	NA
5	7	181.5	59.7	12.0	2.5	NA	NA
	2	#N/A	#N/A	#N/A	#N/A	1.4	0.056
	6	#N/A	#N/A	#N/A	#N/A	1.3	0.053



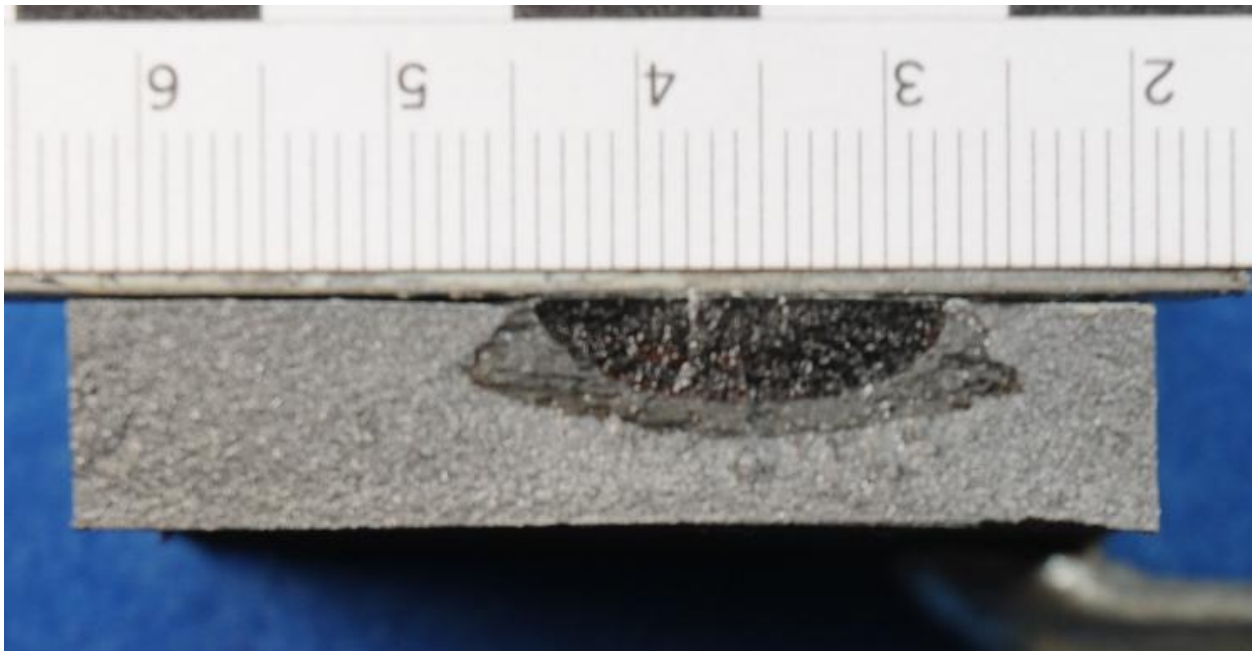
Pipe 13: MPI photo of SCC colony with MWM numbering (blue)



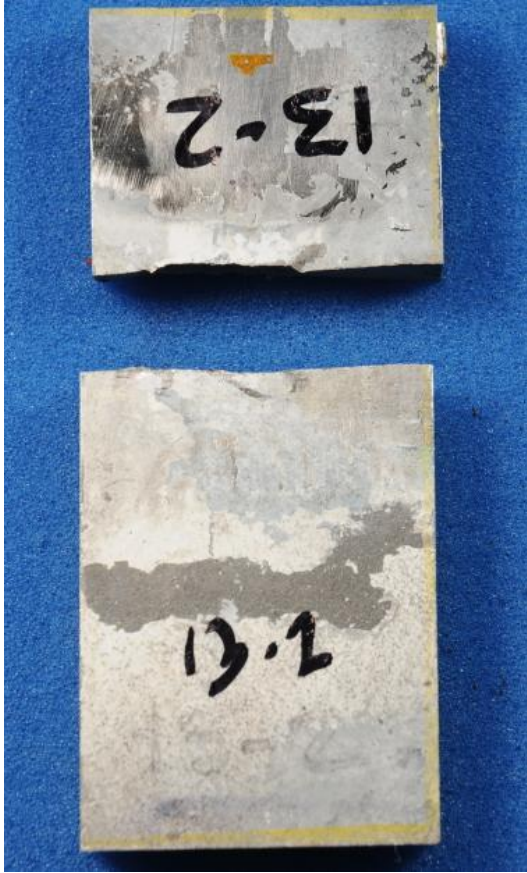
Pipe 13: Fracture surface at MWM 3 leak location (1598 psi), frozen using liquid nitrogen and broken.



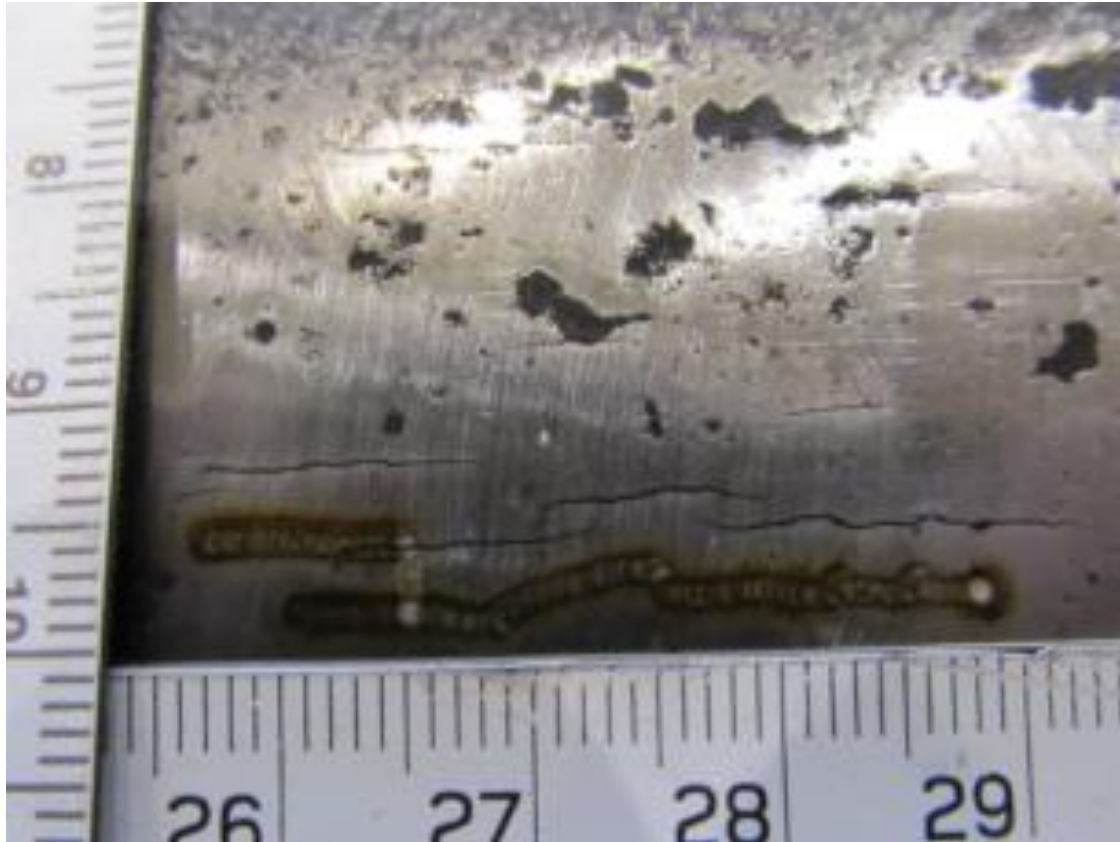
Pipe 13: MWM location 3 after leak at 1598 psi



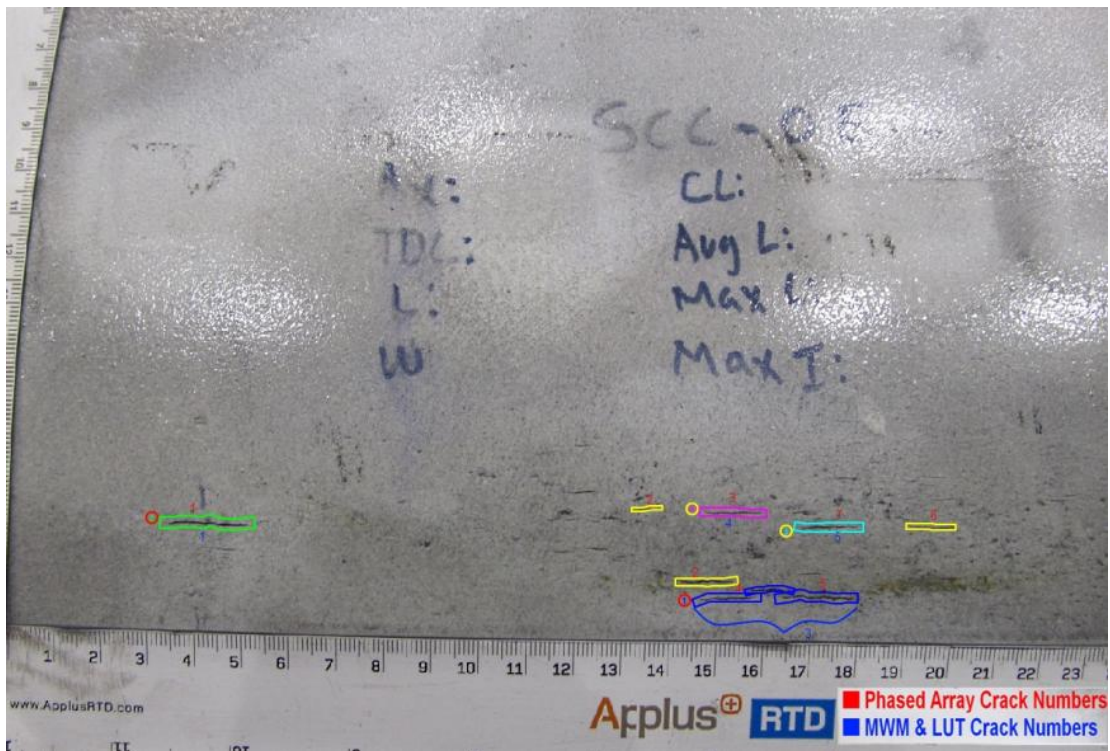
Pipe 13: location 13A after leak at location MWM 3 at 1598 psi



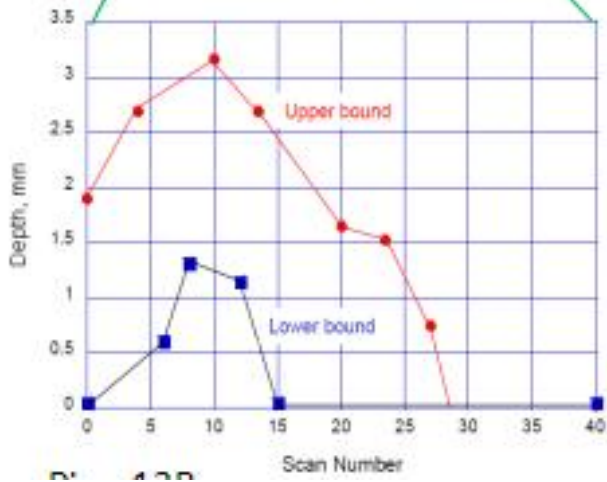
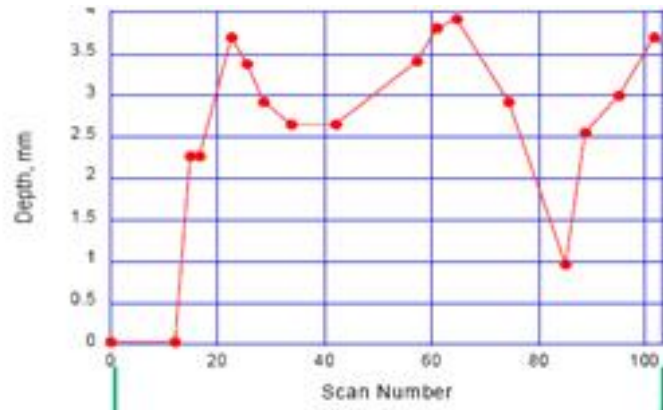
Pipe 13: Location 13A after leak at location MWM 3 at 1598 psi



Pipe 13: LToFD tracking (ablation track) of MWM crack 3 and MWM crack 2.



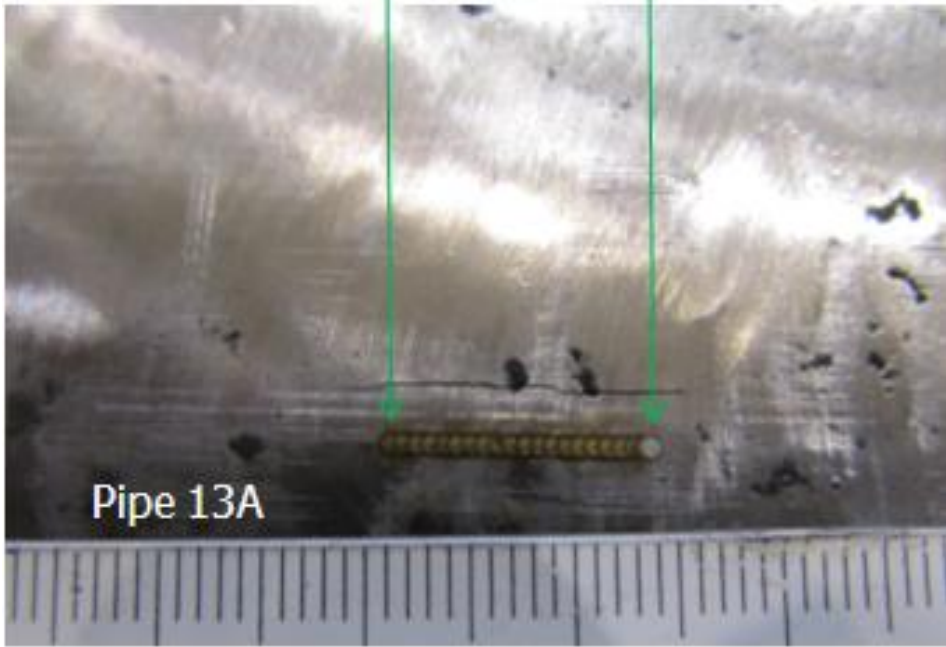
Pipe 13: NACE crack interaction program tracks overlain on MPI photograph



Pipe 13: LToFD sizing at target location, 13-C that leaked at 1598 psi and loc B.



Pipe 13A



Pipe 13: LToFD sizing opportunity at location 13-A (MWM 1)